

**Controlled Deformation of Critical Truss Members Using  
Magnetorheological Dampers with Reversed Power Requirements**

by

Joseph A. Dowd

Submitted to the Office of Honors Programs and Academic Scholarships  
Texas A&M University  
in partial fulfillment of the requirements for  
1998-99 UNIVERSITY UNDERGRADUATE RESEARCH FELLOWS PROGRAM

April 15, 1999

Approved as to style and content by:

---

Prof. Paul N. Roschke, Faculty Advisor  
Department of Civil Engineering

---

Susanna Finnell, Executive Director  
Honors Programs and Academic Scholarships

## TABLE OF CONTENTS

ABSTRACT	1
I. BACKGROUND	2
II. APPLICATION OF REVERSE MAGNETORHEOLOGICAL DAMPERS	3
III. FUZZY LOGIC CONTROL	7
IV. NEURAL NETWORK SPECIFICATION OF CURRENT	12
V. CREEP POTENTIAL AND DESIGN OF A MAGNETORHEOLOGICAL DAMPER WITH REVERSE POWER REQUIREMENTS	19
VI. INVESTIGATION OF CREEP IN A SIMULATED BYPASS DUCT	21
VII. CREEP RESISTANT MR FLUID	24
VIII. THREADED CREEP TEST	25
IIX. SUPPORT OF CREEP RESISTANCE IN LITERATURE	29
IX. DESIGN EXAMPLE OF A MAGNETORHEOLOGICAL DAMPER WITH REVERSE POWER REQUIREMENTS	30
X. FUTURE RESEARCH AND CONCLUSIONS	32
XI. ACKNOWLEDGEMENTS	34
XII. REFERENCES	35
XIII. BIBLIOGRAPHY	38
XIV. APPENDIX	40
A. COMPUTER CODE	40
B. EXPERIMENTAL PLOTS	57

# **Controlled Deformation of Critical Truss Members Using Magnetorheological Dampers with Reversed Power Requirements**

Joseph A. Dowd

**ABSTRACT:** A magnetorheological (MR) damper exhibits a variable damping coefficient depending on the strength of an accompanying magnetic field. A high magnetic field creates a nearly unyielding damper filled with a semi-solid fluid while no magnetic field produces an ordinary viscous damper. Presently, these dampers are being used in a variety of ways by supplying power to an electromagnet that causes stiffening of the damper. Reversing these power requirements allows development of new and innovative applications for MR dampers. For example, ephemeral deformation of critical truss members may be controlled through a reverse MR damper.

The goal is to provide protection to truss structures during severe loading events. Implementation of a reverse damper for an application such as this presents two major tasks: (1) development of a control algorithm and (2) design of an MR damper with reverse power requirements. A control algorithm for dynamic response that uses fuzzy logic and neural networks is presented. A potential design for a reverse MR damper utilizing a combination of permanent magnets and electromagnets is also presented. It is further shown that design for MR dampers with reverse power requirements will be governed by minimization of detrimental effects due to creep of the damper under sustained static loading.

## I. BACKGROUND

A magnetorheological damper with traditional power requirements (see FIG. 1) resembles an ordinary dashpot or viscous damper, but it is filled with magnetorheological (MR) fluid and has an electromagnetic coil wrapped around its piston head. The key uniqueness of an MR damper lies in the properties of the MR fluid. The fluid consists of a carrier medium such as oil or water that contains very small magnetically polarizable particles allowing the properties of the fluid to drastically change with the strength of an accompanying magnetic field (Dyke *et al.*, 1996). Thus, when no current is supplied to the coil wrapped around the piston head, the MR damper behaves as an ordinary viscous damper. However, when current is sent through the coil allowing it to produce a magnetic field, the MR fluid subjected to this field becomes semi-solid (Carlson *et al.*, 1996b; Dyke *et al.*, 1996; Dyke *et al.*, 1998; and Spencer *et al.*, 1997b).

This phenomenon occurs as a result of particles that are suspended in the fluid lining up parallel to the direction of the magnetic field in chain-like structures (*Rheonetic...*, 1998). The yield strength of the damper is directly proportional to the magnitude of the magnetic field and, thus, the amount of current supplied. Forces between particles in the chains control the strength of the fluid. As a result of the potential for these chains to break, an MR damper behaves in two domains. The pre-yield region applies to behavior prior to breaking of the particle chains. Conversely, the post-

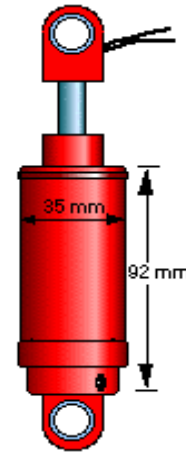


**FIG. 1. Linear MR Damper – Lord Corp.**

yield region applies to behavior after the particle chains have broken. These MR damper characteristics may be exhibited with little use of power. A small battery is perfectly sufficient to completely reverse properties of the fluid within milliseconds when the magnetic field is altered (Dyke *et al.*, 1996).

These advantages of MR damper technology have led to numerous commercial applications and experimental endeavors. Products currently on the market range from exercise equipment to semi-active controlled seat suspension systems for large vehicles (Carlson *et al.*, 1996b). MR dampers are present in seismic control experiments around the world. In an alternate study, Texas

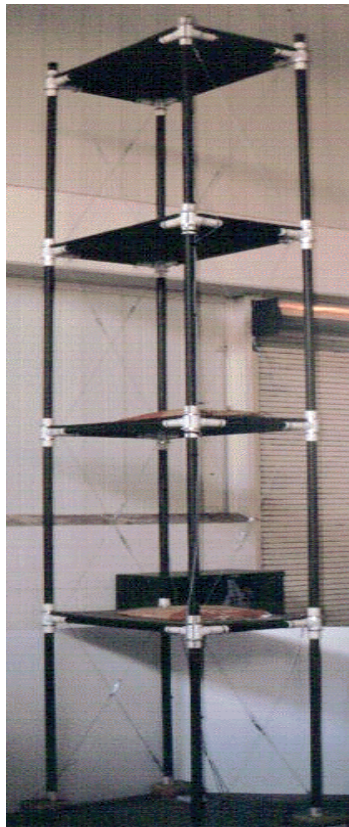


**FIG. 2. Model High-Rise Building**

A&M University is currently embarked on a project to mitigate the effect of wind on high-rise buildings. While the sway of such a building may not be structurally damaging, it can be disconcerting to occupants who may not be convinced of their safety or are nauseated by the motion. To aid the experimental investigation, MR dampers are being installed between floors in a model high-rise building to control inter-story drift (see FIG. 2). Researchers at Texas A&M have also investigated controlling MR dampers placed in the suspension systems of railtrucks in order to protect new automobiles from damage during railway transport. Additionally, they have recently broached the concept of retrofitting one hundred-year-old iron railroad trestles with MR dampers to control vibration caused by passing trains. These projects require control algorithms that take measured structural

responses to external loads and produce the proper control force correction (Soong, 1990). In the case of a high-rise building, accelerometers will be placed on each floor, and measurements from these transducers will be used to control the current supplied to the MR dampers and thus the yield strength of the fluid.

In the current state of technology the MR damper with traditional power requirements behaves passively until an electric current is introduced that creates a magnetic field. This field alters properties of the MR fluid and stiffens the damper. In its inactive state the device is simply a passive viscous damper, while its active state involves varying degrees of stiffening.

In the proposed "reverse" mode that is described in what follows, the damper is in its stiffest condition until an electric current is introduced that softens the device. The inactive state of the reverse device is a stiffness element while its active state involves varying the degree of softening.

## **II. APPLICATION OF REVERSE MAGNETORHEOLOGICAL DAMPERS**

Many problems exist in civil engineering structures comprised of truss members where detrimental stresses within a member are caused by large loads. The resulting stress can be relieved if a support is allowed to temporarily settle or if the critical member is allowed to transiently deform, through elongation or compaction, without incurring the additional stress normally attributed to such a strain. Of course, if a truss is designed correctly, this problem and these solutions should not be necessary under typical design loads. However, a rare event such as an earthquake, hurricane, explosion, or tsunami that produces abnormal loading can cause concern for survival of the structure. To robustly design for these rare loading events as if they were daily occurrences would be

impractical and expensive. Therefore, to be able to relieve stresses in critical members can be very beneficial. Ordinarily, deformation of a linearly elastic truss member is accompanied by a proportional change in the force within the member (see Equation 1).

$$\delta = \frac{PL}{EA} \quad (1)$$

where  $\delta$  = deformation,  $P$  = axial force,  $L$  = length,  $E$  = Modulus of Elasticity, and  $A$  = area.

Load causes a deformation that, in turn, results in an internal force within a member. When loading supercedes a critical level and continues to augment the deformation, the accompanying increase in force is not desirable. Temporary deformation free from the additional concomitant force mandated by Equation 1 may be accomplished using a reverse MR damper that acts as an agent to relieve stress in critical members. The resulting truss will be more resistant to severe loading events that may cause the collapse of a normal truss structure.

To most effectively convey the benefits of controlled deformation of truss members using MR dampers, an example is helpful. When a simple truss (see FIG. 3) is loaded as shown the

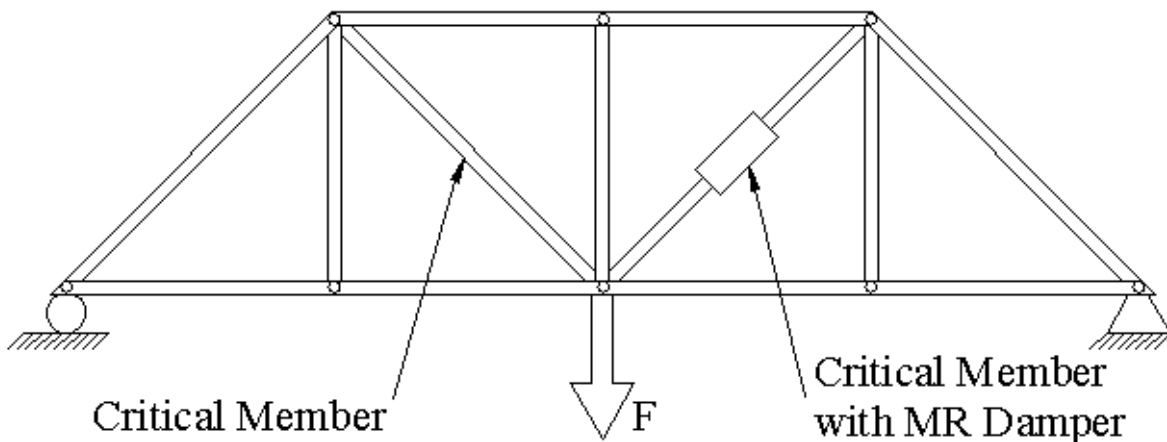


**FIG. 3. Example Truss with Critical Members and MR Damper**

elements labeled as critical members accrue large axial forces. If the force within a critical member produces a stress exceeding the failure stress of the member, it will yield or rupture. This, in turn, could lead to collapse of the structure. This member should be sized so that this condition will not be experienced under design loads. However, should an unusually severe and unanticipated load occur, the structure should still be able to survive despite the fact that the truss was not specifically designed for the rare loading event. Functionality, practicality, and economy all prevent a standard member from withstanding such a force; however, the goal in what follows is to propose a method to increase favorable characteristics of critical truss members under dynamic loading using magnetorheological dampers.

Returning to the simple truss example (see FIG. 3), the applied force would result in the cross-brace experiencing tension and a deformation approximately quantified by Equation 1. This direct proportionality reveals that added deformation increases the force within the member. Failure of the linearly elastic member can then be reported as a critical deformation:

$$\delta_{critical} = \frac{P_{critical} L}{EA} \quad (2)$$

where  $\delta_{critical}$  = critical deformation,  $P_{critical}$  = critical axial force,  $L$  = length,  $E$  = Modulus of Elasticity, and  $A$  = area.

An MR damper has the potential to withstand a large force when it is exposed to a sufficiently strong magnetic field. If a maximally stiff linear MR damper (FIG. 1) is installed in series with the critical truss member (see FIG. 3) and a strain gauge is used to monitor the strain, then as the critical deformation is approached, the magnetic field may be decreased allowing axial elongation through the damper. This compliance serves to relieve stress in the member. Additional

deformation supplied by the relaxation of the damper does not create more force within the member as mandated by Equation 1 but rather dissipates energy from the rare loading event and redistributes excess dynamic stress to surrounding members. The MR damper shown in FIG. 1 is capable of dissipating energy at a rate of over 600 watts (Carlson *et al.*, 1996a). Once a final deformation state has been achieved, the high magnetic field may be restored and, in essence, “lock” the member secure again. Then, after the rare loading event is over, the truss may be returned and “locked” in its normal position, or depending on the severity of the event and the pattern of loading, the entire truss may need repair or replacement. In either case, collapse and possible loss of life are prevented.

Insight into the control of dynamic deformation of critical truss members using reverse MR dampers is presented using fuzzy logic and neural networks. The ultimate goal is to provide a means of controlling a reverse MR damper embedded in a truss system as discussed that undergoes stochastic loading conditions. A prototype controller is presented here using a numerical simulation of a truss system and laboratory data gleaned from an MR damper with traditional power requirements.

### **III. FUZZY LOGIC CONTROL**

Fuzzy logic is responsible for the decision making process within the proposed algorithm to control dynamic deformation of critical truss members using an MR damper. Fuzzy logic is used to deal with sets that have unclear boundaries. Jang *et al.* use the example of days of the week. Strictly speaking, the weekend consists of Saturday and Sunday, but Friday night seems more like the weekend than Sunday night. One law of classical sets mandates that something must either be

a member of a particular set or not be a member of this set. Fuzzy logic ignores this crisp definition and assigns a degree of membership to a particular set. Saturday may be a one hundred percent member of the fuzzy set *days of the weekend* while Friday is only a forty-three percent member. Both discrete and continuous fuzzy sets may thus be described by a membership function revealing the degree of membership of a particular random variable to a fuzzy set (Jang *et al.*, 1997).

A fuzzy inference system (FIS) uses fuzzy logic to compute an output based upon given input and the inherent rules and functions of the FIS. Inputs are first fuzzified through the input membership functions and are combined using fuzzy operators that include typical Boolean operators. Order and type of fuzzy operators used are a result of the rules assigned during creation of the FIS. An implication process creates a fuzzy set based upon results of the fuzzy operations and the preset membership functions. A fuzzy set then exists for each of the rules of the FIS. These rule sets are combined by one of several possible aggregation methods to produce a single fuzzified output. This output must then be defuzzified using output membership functions to provide the useable output of the FIS (Jang *et al.*, 1997).

To investigate controlled deformation of a single truss element using a single MR damper (see FIG. 3), the stress of the element was used as the input to a FIS using MATLAB's Fuzzy Logic Toolbox. The input was fuzzified using the membership functions shown in FIG. 4. Five simple rules such as "If 'Normal' then 'MaxStiff'" and "If 'HighTension' then 'MaxSoft'" were chosen to govern the FIS (see Appendix). A "max" aggregation and centroidal defuzzification were used with the output membership functions (see FIG. 5). The defuzzified output of the FIS is a value termed *percent of stiffening capacity* based upon how close the current stress level is to the failure strength

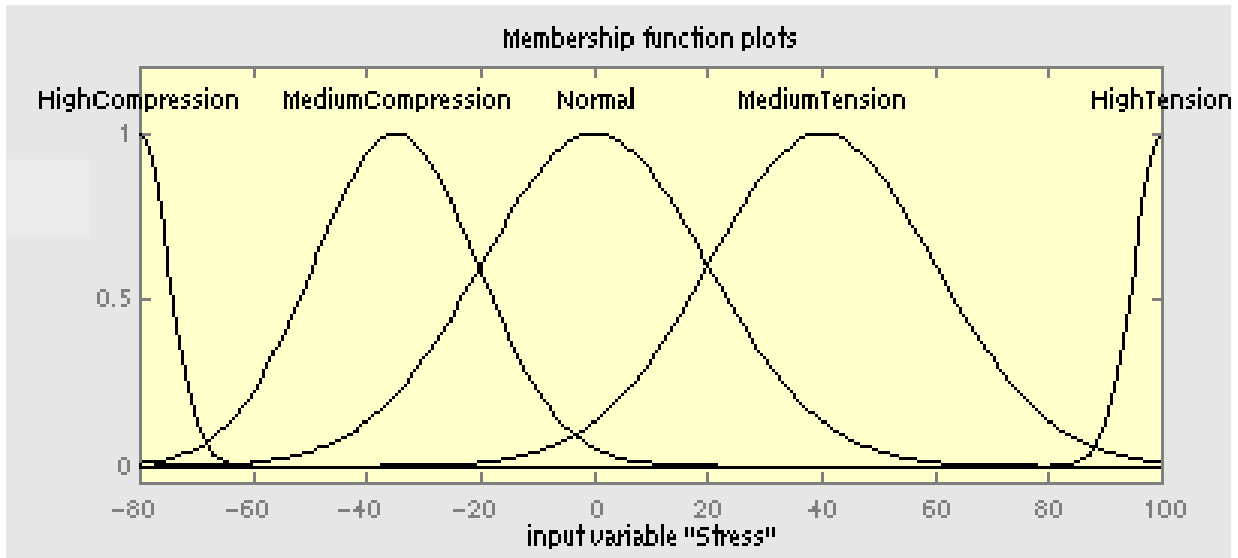


**FIG. 4. Input Membership Functions**

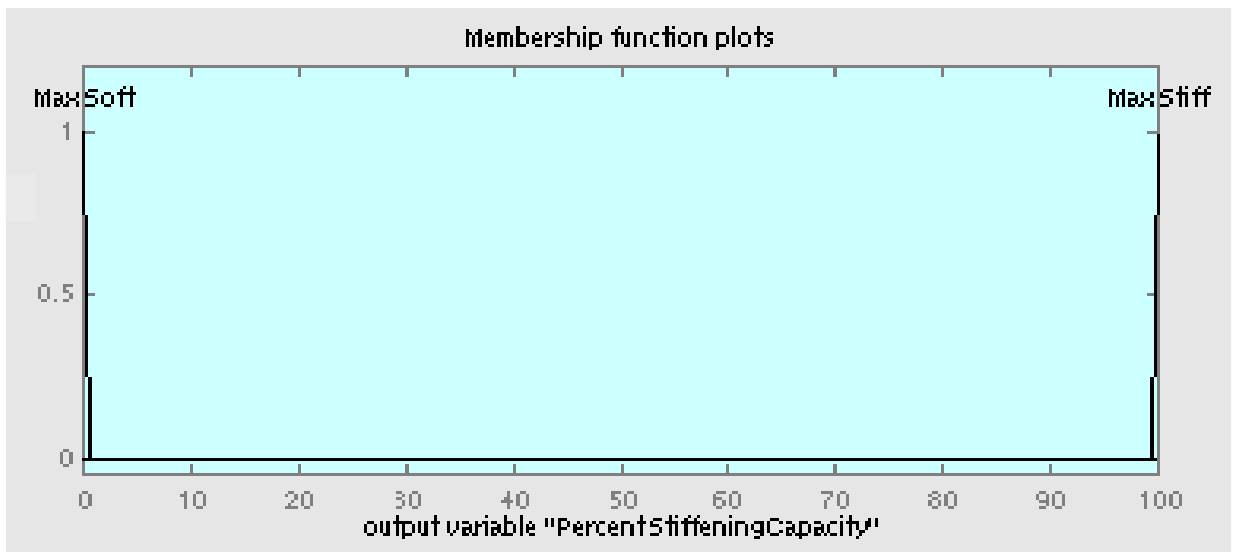


**FIG. 5. Output Membership Functions**

of the member. Notice that the output membership functions are narrow Gaussian spikes at the beginning and end of the range of values. These functions represent the two opposite ends of the operational spectrum of the damper: fully stiff and fully softened.

The FIS is embedded in the Simulink program shown in FIG. 6 and in the Appendix. For simplicity, this FIS only analyzes the degree of freedom of the truss that contains the stroke of the damper. Program inputs include initial stiffness, initial damping, mass, and a variable semi-random displacement as a function of time. The uncontrolled stress as a function of time is calculated and displayed graphically using the following equation of motion:

$$Kx(t) + C\dot{x}(t) + M\ddot{x}(t) = F(t) \quad (3)$$

where  $K$  = stiffness,  $C$  = damping,  $M$  = mass,  $F(t)$  = time dependent force, and  $x(t)$  = displacement as a function of time. Simultaneous to the calculation of the uncontrolled stress, the stress level at a given time step is fed back to the FIS which uses its rules and membership functions to produce the *percent of stiffening capacity*. This percentage is used to decrease stiffness and increase damping of the system thereby simulating the effect that a deformable MR damper might have on the system. With these new values, the controlled stress is calculated as a function of time and displayed graphically. FIG. 7 through 9 show a sample input displacement history accompanied by the *percent*

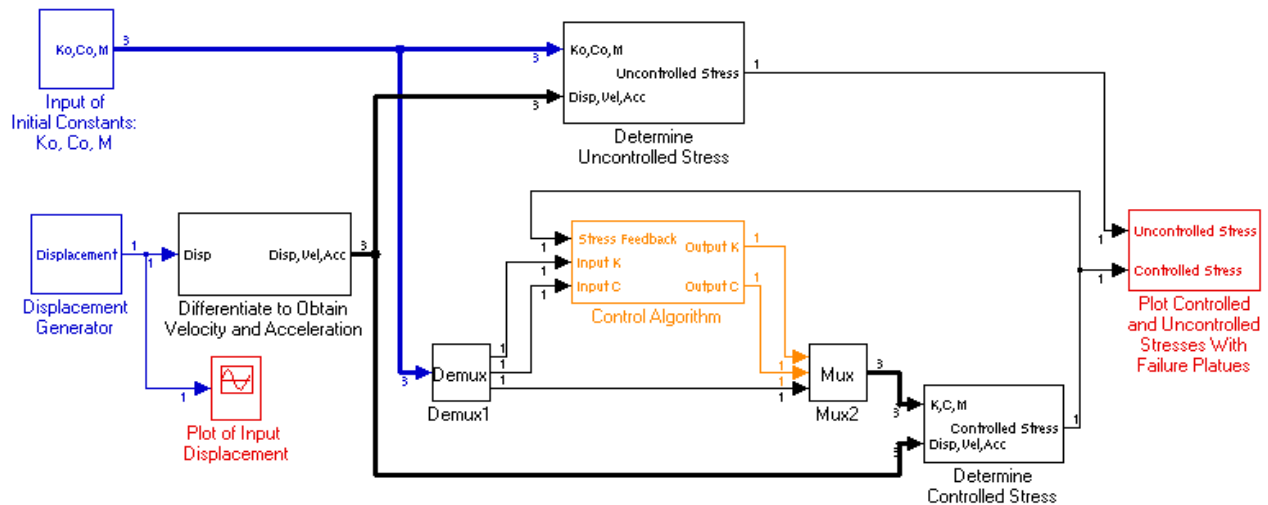
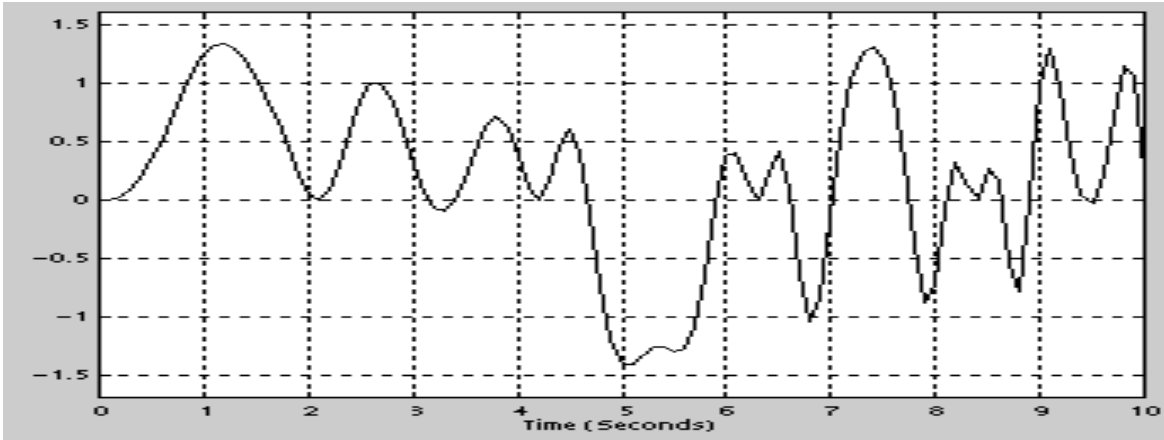
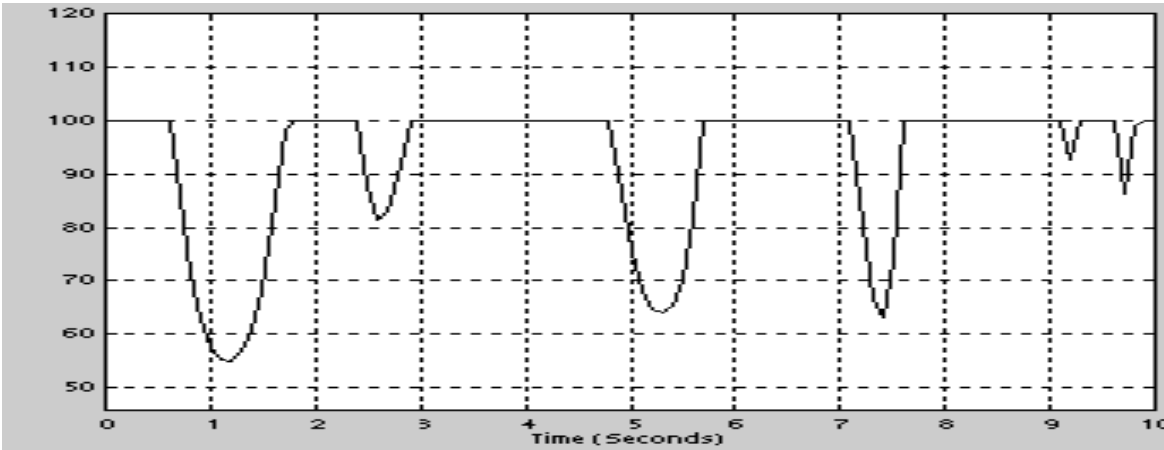


FIG. 6. Simulink Model



**FIG. 7. Input Displacement**



**FIG. 8. Percent of Stiffening Capacity**

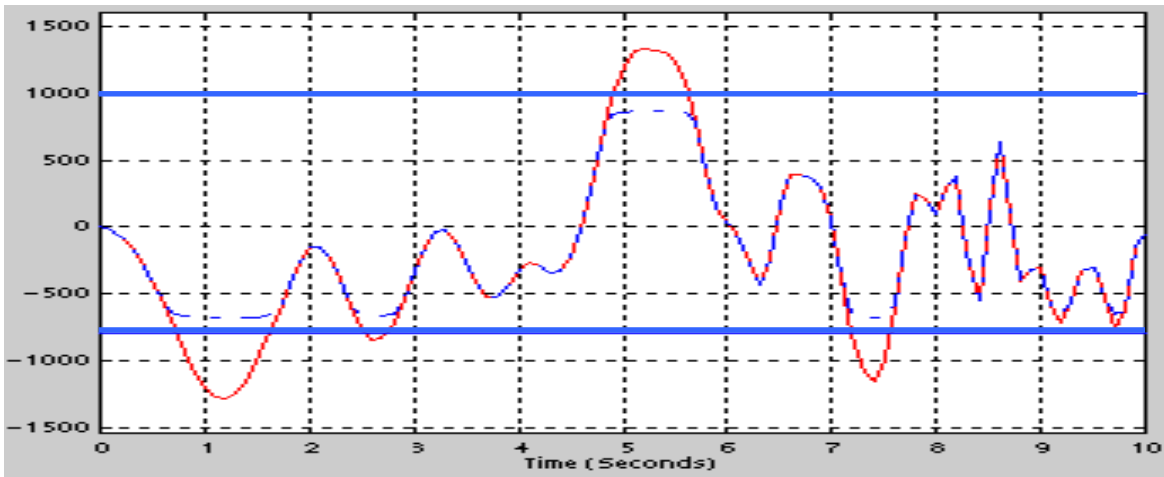


**FIG. 9. Uncontrolled (solid line) and Controlled (dotted line) Stress**

*of stiffening capacity* and the controlled and uncontrolled stresses associated with this displacement. The solid horizontal lines plotted in FIG. 9 represent the failure plateaus associated with tension and compression. Units do not apply in this non-dimensional numerical study, but failure was assumed to occur at 1000 for tension and -800 for compression. The uncontrolled stress reached tensile levels in excess of 1250 and compressive levels below -1000. However, the controlled stress does not exceed 1000 or become less than -800. The numerical analysis shows that although the uncontrolled stress breaches the failure plateaus, the controlled stress is maintained at a safe level.

#### **IV. NEURAL NETWORK SPECIFICATION OF CURRENT**

Although a fuzzy controller appears feasible, the task of translating the desired stiffness of the MR damper into the magnitude of current that is to be supplied to the damper is yet to be discussed. As described in what follows, specification of the current may be accomplished with a neural network.

Neural networks consist of many simple processing units each of which may have multiple inputs and outputs (see FIG. 10). When these units, which are called neurons, are combined, a specific operation may be established (Burton *et al.*, 1996). Elements of the input vector to a particular neuron are combined within the unit. They are based upon assigned weights that correspond to each element of the input vector. The combination is then summed with an assigned bias value that is translated to a single output based upon any one of a number of possible transfer functions. The neurons are combined into hidden and output layers so as to create a network architecture that performs a specific task such as classifying data or approximating functions. A

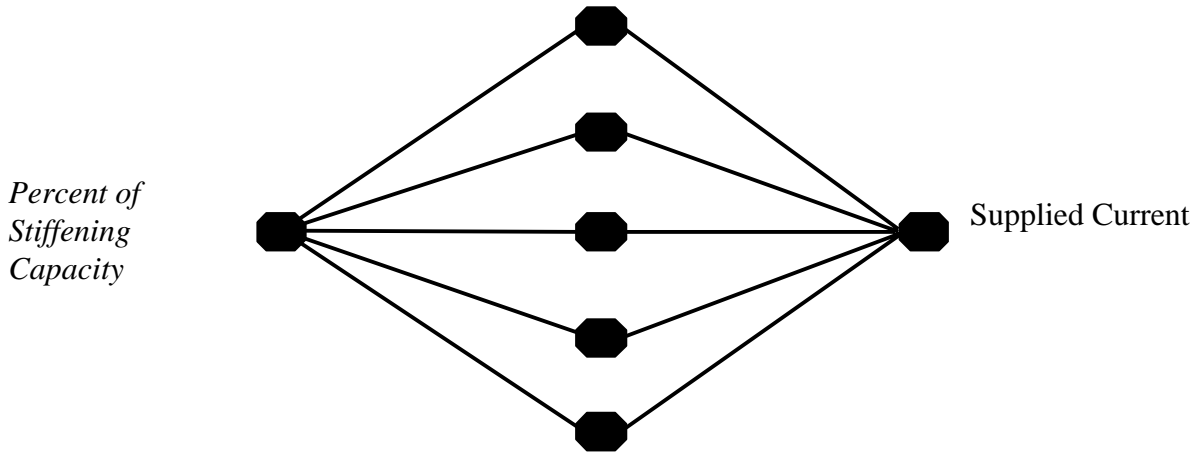


**FIG. 10. Neural Network Architecture**

network is trained to execute its assigned duty through adjustment of the weights and biases of the individual neurons (Demuth *et al.*, 1997).

A neural network is used here to transform the *percent of stiffening capacity* provided by the Fuzzy Inference System into a necessary current to be provided to the MR damper in order for the MR damper to exhibit the required characteristics. A basic two-layer neural network architecture was established to relate *percent of stiffening capacity* to current (see FIG. 10). The hidden layer contains five neurons each using a tan-sigmoid transfer function. The output layer consists of a single neuron with a *purelin* linear transfer function.

An essential element in the creation of a neural network is the existence of reliable data with which to train the network. Training data needed in this case consists of the equivalent stiffness of a typical MR damper and a corresponding spectrum of applied currents. It is assumed that the equivalent stiffness of the damper is a combination of the effects produced by a decrease in stiffness and increase in damping that is simulated in the Simulink model.

The definition of equivalent stiffness varies in archival literature. Pang *et al.* (1998) obtain

an equivalent stiffness,  $K'$ , of an MR damper using the cosine and sine Fourier coefficients of the damper displacement,  $X_{1C}$  and  $X_{1S}$ , and the excitation force,  $F_{1C}$  and  $F_{1S}$ , at specific frequencies of excitation:

$$K' = \frac{F_{1C} X_{1C} + F_{1S} X_{1S}}{X_{1C}^2 + X_{1S}^2} \quad (4)$$

Other researchers relate equivalent stiffness to maximum accumulation of energy or shear stress (Dejiang *et al.*, 1997).

However, these methods are inapplicable to the determination of an equivalent stiffness for training of this neural network. For example, Equation 4 may only be used for a constant frequency, while the neural network here will be used for stochastic excitation. Other methods use all of the data obtained from a series of complete damper strokes. This includes both pre-yield and post-yield regions of the behavior of the MR fluid. Using a completely rigid MR damper as a stiffness element (such as with the controlled deformation of truss elements) means that the MR damper behaves entirely within the pre-yield domain. Thus, the training of a neural network to be used in this application should use values for equivalent stiffness obtained solely from this pre-yield region where the chain structures in the MR fluid have not been broken.



**FIG. 11. MTS Testing of MR Damper**

To this end, eleven sets of displacement and force data were obtained from a uniaxial test in an MTS machine using a small prototype MRWD-002 light-duty damper with traditional power requirements obtained from Lord Corporation (see FIG. 11). A sinusoidal displacement with an amplitude of 1 mm and a frequency of 0.5 Hz was tested at eleven different levels of applied current that subdivide the range from 0.0 to 1.0 amp as shown in TABLE 1. The low frequency and amplitude ensured that the velocity remained low, which is similar to what might be experienced in a civil engineering application. Plots of displacement versus force and velocity versus force were prepared for each data set (see Appendix). As an example, the graphs of displacement and velocity versus force for 0.3 amps of applied current are exhibited in FIG. 12 and 13

In order to isolate the pre-yield region, the plot of velocity versus force was analyzed for each value of applied current. The semi-horizontal lines at each of the two extremes of the hysteretic loop represent the post-yield region. The region of the plot passing near the origin connecting these two plateaus comprises the pre-yield region. The data set associated with each level of applied current produces a different range of forces that spans the pre-yield region. This same range of force values

<b>TABLE 1. Training Data for Neural Network</b>				
<b>DATA SET</b>	<b>CURRENT (amps)</b>	<b>SLOPE MAGNITUDE</b>	<b>EQUIVALENT STIFFNESS (kN/cm)</b>	<b>PERCENT OF STIFFENING CAPACITY</b>
1	1.0	11.996	140.05	100.00%
2	0.9	11.838	138.20	98.68%
3	0.8	10.801	126.10	90.04%
4	0.7	9.654	112.71	80.48%
5	0.6	7.936	92.65	66.16%
6	0.5	7.372	86.06	61.45%
7	0.4	6.552	76.49	54.62%
8	0.3	5.855	68.36	48.81%
9	0.2	5.152	60.15	42.95%
10	0.1	4.666	54.47	38.90%
11	0.0	2.143	25.02	17.87%

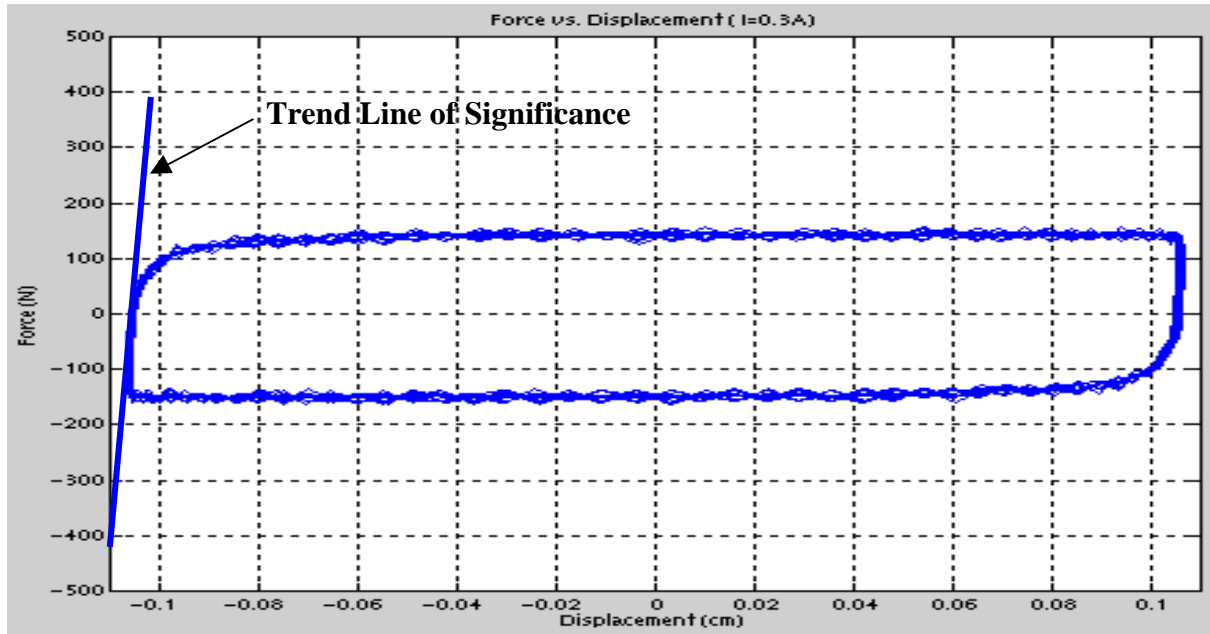


**FIG. 12. Displacement Versus Force for 0.3 Amps**

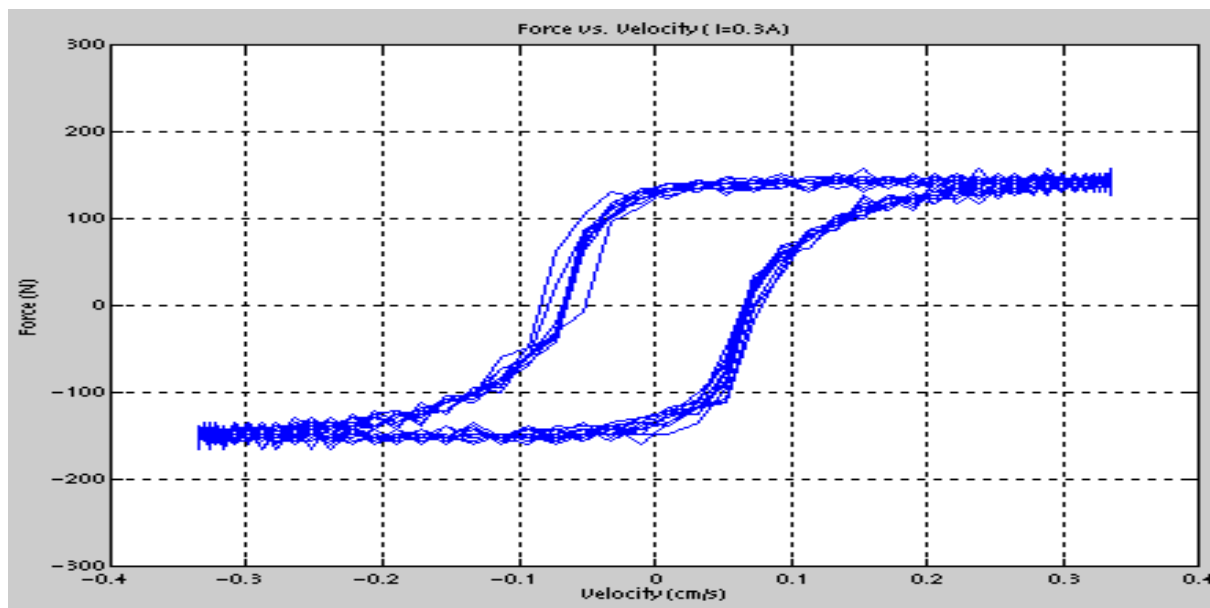


**FIG. 13. Velocity Versus Force for 0.3 Amps**

associated with the pre-yield region may be identified on a plot of displacement versus force such as that shown in FIG. 12. By filtering out points not falling in this range, the slope of the displacement-force relationship in the pre-yield region may be determined. That is, it is proposed

that the slope of a trend line through the pre-yield data points represents the equivalent stiffness of the pre-yield region of the MR damper (FIG. 12).

The equivalent stiffness increases in a nonlinear fashion as the level of the current applied to the MR damper is augmented (see FIG. 14). These data points are used to train the neural network to correctly predict the applied current that is necessary to produce the desired stiffness. It should be noted that these values of equivalent stiffness are all obtained from sinusoidal tests with identical frequency and amplitude. It is possible that varying frequencies or amplitudes of the applied motion could result in different values for the equivalent stiffness. In addition, determination of the range of force values associated with the pre-yield region in this analysis is very objective. Increasing or decreasing the range of allowable force values for each level of applied current has a direct effect on the slope of the remaining line and thus has an effect on the obtained value for equivalent stiffness. In short, the approach used here is meant to be demonstrative and not definitive. A trend between applied current and equivalent stiffness was identified while holding all other factors constant. A major advantage for use of a neural network is that if the equivalent stiffness is found to rely on additional factors such as velocity or acceleration, these factors may simply be added as supplemental inputs to the network. The network could then be retrained using the appropriate experimental data.

Additionally, data used to train the neural network apply only to the damper from which it was acquired. Recall that data used to train this network comes from an MR damper with traditional power requirements. This is necessary due to the fact that an MR damper with reverse power requirements does not yet exist. In order for a neural network to be used in an actual application such as controlling deformation of truss members, it would have to be trained with data not only

from a reverse MR damper, but specifically from the particular reverse MR damper to be used. This is necessary because each damper may exhibit slightly different traits. However, neural networks have been shown to provide efficient characterization of an MR damper (Zhang *et al.*, 1998).

In order to embed the neural network trained here in the Simulink model containing the fuzzy control algorithm presented earlier (see FIG. 6), the stiffness data was normalized. Each stiffness value was divided by the largest stiffness value, which was obtained at an applied current of 1.0 amps (see Table 1). The result is a *percent of stiffening capacity* exhibited by each level of applied current. The Levenberg-Marquardt algorithm (*trainlm*) was used to train the network (see FIG. 10) in a small number of cycles using the normalized stiffness and current data. FIG. 14 shows the normalized stiffness data along with the neural network output for a range of applied current. The

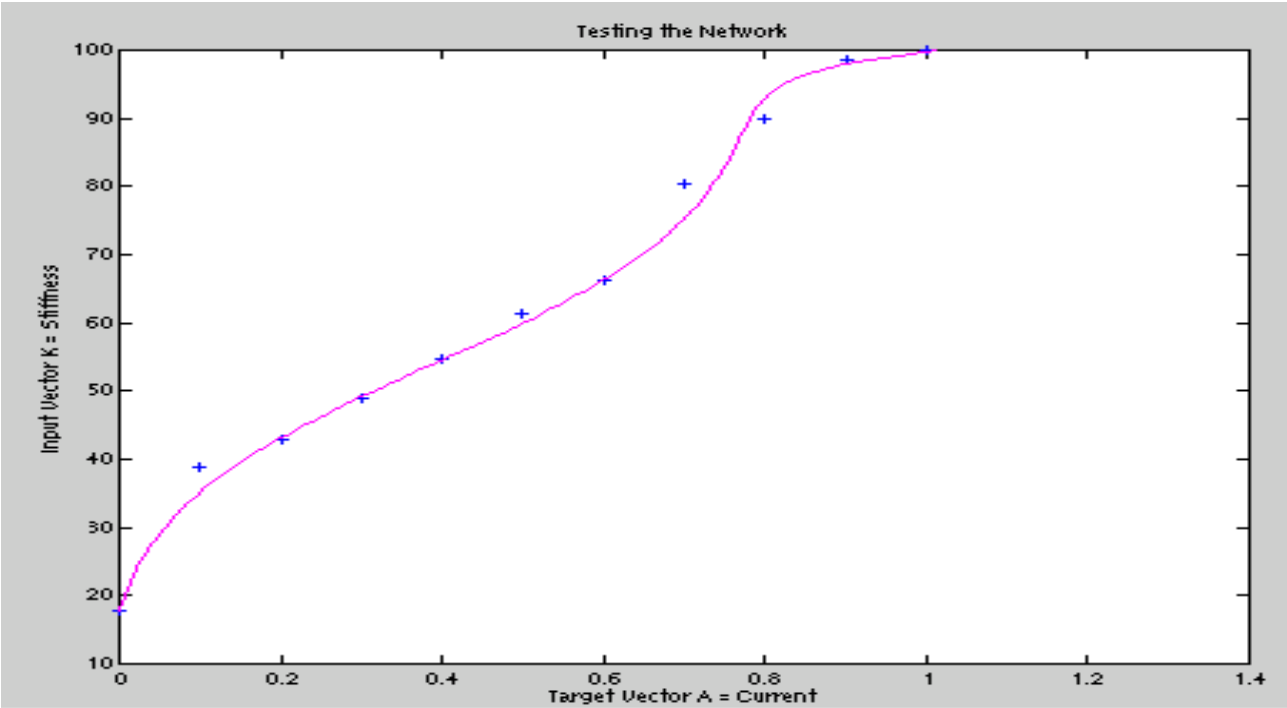


**FIG. 14. Neural Network Output Predicting *Percent of Stiffening Capacity***

resulting neural network was embedded into the Simulink model presented earlier (see FIG. 6). It should be noted from FIG. 14 that the lowest attainable *percent of stiffening capacity* is approximately 18%. Therefore, the control algorithm was directed not to allow a value less than this to be delivered to the neural network (see Appendix). Using the same input displacement as FIG. 7, a plot of the required current is generated for the loading scenario (see FIG. 15). As per the definition of a reverse MR damper, the status quo has a current of approximately one amp, with a decrease in the magnitude of current when softening of the device is necessitated. This represents

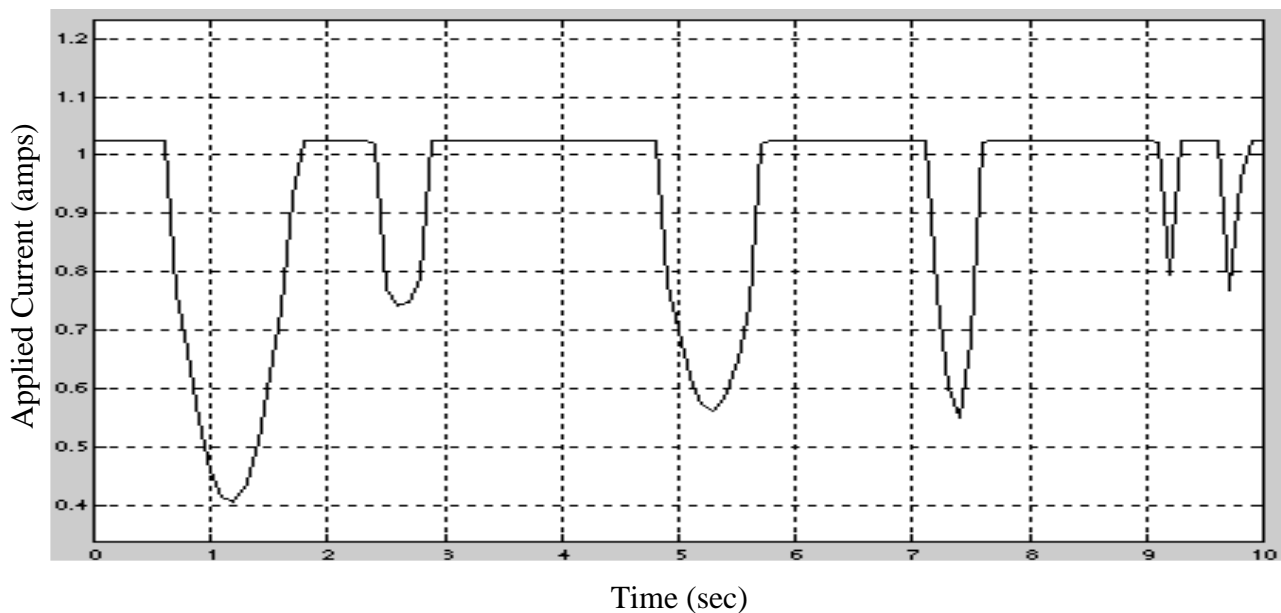


**FIG. 15. Time History of Desired Current**

the controlling action necessary to allow the MR damper to prevent failure of the truss member by a controlled level of deformation.

## **V. CREEP POTENTIAL AND DESIGN OF A MAGNETORHEOLOGICAL DAMPER WITH REVERSE POWER REQUIREMENTS**

Availability of a reverse MR damper has been assumed in the previous sections. In order for the MR damper to remain semi-solid and “locked” as part of a critical truss member and thereby allow the truss to behave as a stiff structure under ordinary loading conditions, constant power for an electromagnet is demanded. This presents two major concerns. First, an application such as this would be an inefficient use of power despite the relatively low power requirements of an MR fluid. The second is less an issue of cost efficiency or power conservation and more an issue of danger. Since current uses for MR dampers allow them to act passively as ordinary viscous dampers most of the time, a power outage or any damage to the power supply of the damper does not result in a catastrophe. This is not the case here. Anything preventing power from supplying the coil with current prevents formation of a magnetic field. This inhibits the ability of the damper to remain “locked,” and a critical truss member with an MR damper would be rendered ineffective as an element of its truss system. In an extreme case, this could cause collapse of the structure under ordinary loading conditions. Both problems may be rectified through the design of an MR damper with reversed power requirements.

First, there is a concern as to whether or not an MR damper will behave as desired in a one hundred percent stiff or “locked” situation. It can be argued that even though the damper contains fluid in an almost solid state in the presence of a significant magnetic field, it is still a damper and thus governed by the fundamental relationship that force equals velocity times the damping coefficient. In light of this fact and taking into consideration that for the application at hand the velocity will be zero for a significant amount of the time, it is necessary to determine if a “locked” MR damper creeps under a sustained load

An attempt to determine the creep resistance of a variety of reverse MR damper designs was executed. Preliminary testing on a linear MR damper (see FIG. 16) resulted in significant creep under a sustained load. This may be a trait of the current design of MR dampers.

## VI. INVESTIGATION OF CREEP IN A SIMULATED BYPASS DUCT

MR dampers are not presently designed to be operated in a “reverse” mode. The area of fluid that becomes solidified due to application of a magnetic field forms a relatively small annular ring around the piston head. For example, one MR damper currently in production contains  $70 \text{ cm}^3$  of MR fluid but has only about  $0.3 \text{ cm}^3$  of fluid affected by the magnetic field at any given time (Jolly *et al.*, 1998). This design may lead to slippage between the solidified MR fluid region and the piston head or cylinder wall. This slippage may be prevented with a change in design that borrows concepts from electrorheological (ER) dampers.

Fluid in an ER damper is similar to MR fluid except that it displays a variety of characteristics in the presence of an electric field rather than a magnetic field. An ER damper design presented by Burton, *et al.* (1996), and Makris, *et al.* (1996), does not allow fluid to flow past the piston head. Instead, the ER fluid flows through a stationary duct that bypasses the piston head in



**FIG. 16. Simple Creep Test**

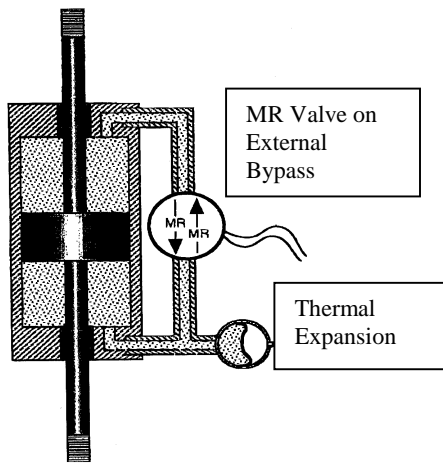


**FIG. 17. MR Damper Featuring Bypass Duct - Lord Corp.**

which the fluid is exposed to an electric field. It is conceivable that an MR damper can be designed in a similar fashion. An MR damper with a bypass duct being investigated by the Lord Corporation is shown in FIG. 17. It is possible to solidify a section of MR fluid in a region of this duct that varies in cross-section as in FIG. 18. This would prevent the solidified fluid from slipping against the walls of the duct. Therefore, the only feasible shear failure mechanism allowing creep would be a shear failure

plane within the MR fluid mass itself.

A creep test investigating the plausibility of this theory was conducted as shown in FIG. 18. A 9.5-mm (3/8-in.) inner diameter tube was attached to an air bladder. A 9.5-mm (3/8-in.) outer diameter tube was glued to the inside of the end of the larger tube. This created a neck in the area of flow within the tubes where the diameter decreases. This region was filled with MRF-132LD MR fluid obtained from Lord Corporation in an effort to reproduce the region of a bypass duct that changes cross-section. A permanent magnet was placed beside this segment of tubing thereby solidifying this region of fluid. Air within the bladder was pressurized with weights producing a force on the MR fluid in the tubing. The test apparatus simulates a maximally stiff MR damper with a bypass duct under sustained loading.

As a preliminary test, the apparatus was maintained in a loaded position for approximately eighty-two hours with no visible flow of the fluid. The permanent magnet was removed, and the MR fluid promptly ran out of the tubing. Following the liquid was a continuous exhaust of air indicating



**FIG. 18. Region of Bypass Duct Varying in Cross-Section**

that the testing method and apparatus were effective.

In a real application a reverse MR damper needs to sustain a load for a period of time that is significantly longer. Therefore, a second test was conducted that possessed a duration of approximately one month. The long-term test provided some surprising results. The level of MR fluid in the tube changed slowly, denoting slight fluid flow and, thus, creep. However, the only fluid that exited the tube was the carrier fluid, oil. In addition, significant settlement of the magnetizable particles from the carrier fluid was observed in the regions of the tube away from the magnetic field. The volume of carrier fluid on the top of the MR fluid column within the tube appeared to be decreasing as the height of the column decreased. Thus, only carrier fluid escaped. It can be argued that this is consistent with the literature. Jolly *et al.* (1998) and others maintain that yielding of the fluid in the semi-solid state depends on yielding and breaking of the chains of magnetically polarizable particles. It is plausible that the chains in this long-term creep test were not being broken, but rather, the carrier fluid was simply flowing around the chains. This theory is supported by behavior of the carrier fluid in this experiment. The chain structures in the solidified MR fluid were found to be permeable. Thus, the long-term creep test simulating an MR damper with a variable cross-section bypass duct revealed problems with the design but also provided valuable information

allowing new ideas to be explored.

## VII. CREEP RESISTANT MR FLUID

The fact that the mechanism for creep in the long-term test did not involve yielding of the chains implies that an MR fluid may be specifically tailored towards creep resistance in the form of chain permeation. Several different types of MR fluids are commercially available. Characteristics such as carrier fluid, plastic viscosity, and compatibility with rubber vary widely. These variations make the fluids suitable for different applications. For example, as the percentage of iron by volume of the fluid increases, the viscosity increases, the initial settling rate decreases, and the fluid can sustain more magnetic flux before becoming saturated (Jolly *et al.* 1998). These three characteristics and the direction of their trends support the possibility of an MR fluid with greater creep resistance. Higher viscosity denotes less rapid flow. A slower settling rate suggests that the carrier fluid may be less inclined to flow between the chain structures, and the higher magnetic flux suggests a stronger bond within and between these particle chains. It is unknown as to how much an increase in viscosity of the fluid as a whole will affect creep since viscosity of an MR fluid tends to increase with decreasing shear rates (*MRF-132LD*, 1998). However, a carrier fluid with higher independent viscosity may impede the form of creep through chain structure permeation.

Additionally, researchers around the world are developing new MR fluids. Margida *et al.* (1996) have tested fluids composed of non-typical iron alloys that provide differing yield stresses based upon elemental composition. Kordonsky *et al.* (1996) have added magnetorigid particles to a typical MR fluid. They have displayed a fluid that behaves as a normal MR fluid outside of a

magnetic field but has a field-dependent viscosity almost an order of magnitude greater than a typical MR fluid. Other variations are possible, but the intent is to demonstrate that improvements are being made that make solidified MR fluid less permeable thus creating a creep resistant MR fluid and damper.

### **VIII. THREADED CREEP TEST**

The long-term creep test simulating an MR damper with a variable cross-section bypass duct also revealed a difficulty with trying to prevent motion of the piston head *indirectly*. Motion is indirectly prevented through solidification of the bypass region, but it was seen that this is overcome by the permeability of the chain structure. The traditional MR damper design that was originally tested *directly* prevents the piston head from relocating because the solidified region of MR fluid surrounds the moving part. This gives control of the strength of the damper back to the strength of the chains themselves. However, the problem with the design is the possibility of slip along the contact surfaces. This, too, may be remedied. Tang *et al.* (1996) found that if slip is prevented, an MR fluid's maximum shear stress may be increased 6-fold. In their experiments, a model MR fluid in which the lead particle of each chain was glued to the shearing wall was compared to the same fluid with no particles fixed to the walls. These researchers reported that the attraction between MR particles is higher than the attraction between an MR particle and the wall. However, the attractive force between an MR particle and the wall becomes approximately twice that of the attraction between MR particles when the wall possesses a roughness of two to three times the particle diameter. This is extremely significant because it allows an MR damper design that capitalizes on

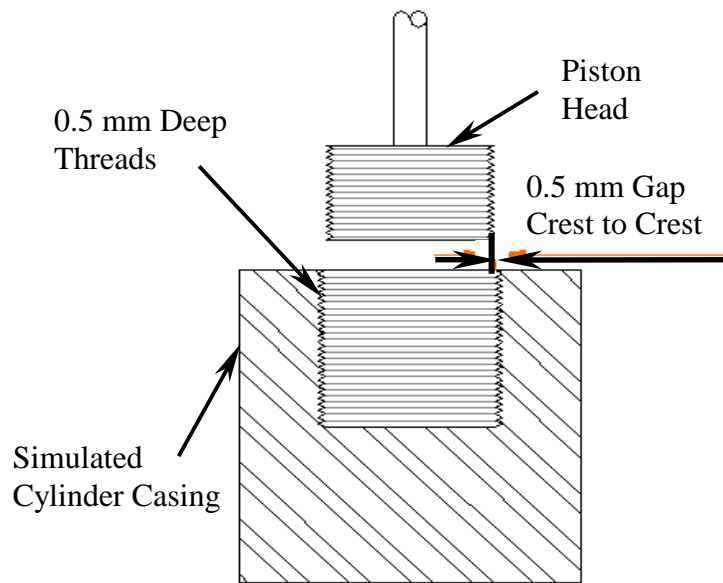


**FIG. 19. Cross-Section of Threaded Creep Test Apparatus**



**FIG. 20. Threaded Creep Test Apparatus**

positive aspects of both designs already discussed: motion of the piston head is directly prohibited *and* slip is prevented.

To test this design, parallel grooves resembling threads were machined around the piston head of an existing MR damper (see FIG. 19). Spaced 0.5 mm apart with a depth of 0.5 mm each, these grooves allow the diameter of the piston head to be 28 mm measured from crest to crest. A 29 mm diameter hole was then bored into a 50 mm long segment of a 76.2 mm (3 in.) diameter carbonized



**FIG. 21. Threaded Creep Test Set-Up**

steel cylinder to simulate the inside of a cylinder casing. This hole was threaded identically to the piston head so that when the piston head is lowered concentrically into the hole an approximately 0.5-mm annular gap exists between the crests of the threads of the cylinder casing piston head.

MR fluid was then placed in the hole so that when the piston head is inserted, the annular gap is filled with fluid (see FIG. 20). A power supply was utilized to provide a constant voltage of 4.60 volts to the wire wrapped around the piston head. This produced a near constant current of approximately 1.0 amp and caused the solidification of the MR fluid. The entire apparatus was then inverted, secured, and loaded with 485 grams of weight hung from the shaft of the piston head (see FIG. 21). A dial gauge was positioned as shown to indicate motion of the piston head. Motion was expected to occur because elongation of chains of MR particles exposed to tension is known to take place through gaps between the particles. Research has indicated, though, that this form of creep

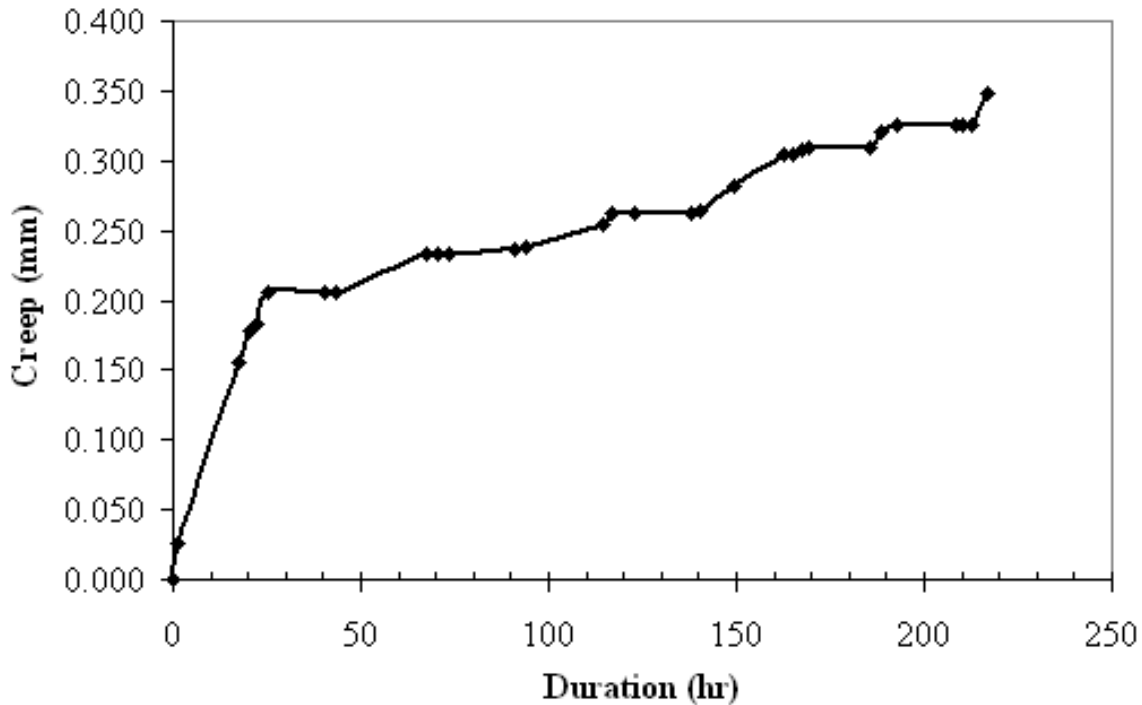


**FIG. 22. Threaded Creep Test Results**

reaches equilibrium (Lemaire *et al.*, 1996). The purpose of this investigation was to determine if creep would continue under constant sustained static load or if it would reach equilibrium as suggested in the literature.

FIG. 22 tracks the creep of the piston head over the 217-hour duration of the test. The first 24 hours shows more than half of the deformation. This can most likely be attributed to the initial deformation of the chains discussed by Lemaire *et al.* (1996). After this point, however, the creep continued at a slower rate. It is unclear whether equilibrium had not yet been attained or if the design itself is not creep resistant. The potential problem with the theory behind this design may lie in the formation of the chains. As normal deformation occurs, gaps between the particles in the chains grow larger until equilibrium is reached (Lemaire *et al.*, 1996). This may allow other particles to enter the chains filling these gaps and making the chains longer in the process. This could

theoretically perpetuate preventing equilibrium from being reached and allowing creep. Researchers such as Liu *et al.* (1996) are still studying the complex topic of chain interaction within MR fluids.

### **IX. SUPPORT OF CREEP RESISTANCE IN LITERATURE**

Despite discouraging results, promising indications toward the possibility of a creep resistant MR damper may be found in literature and in commercially available products. For example, Lord Corporation manufactures the MRB-2107-3 Rotary Brake (see FIG. 23) that is used in such applications as variable resistance exercise equipment. Lord Corporation claims that at 0 rotations per minute, 6.55 N-m (58 lb-in.) of torque may be maintained for as long as 1 amp of current is applied to the coil (*Rheonetic...*, 1998). This implies a scenario involving MR fluid that does not allow creep.

Dyke *et al.* (1996a), Spencer *et al.* (1997a, 1997b), Pang *et al.* (1998), and others show

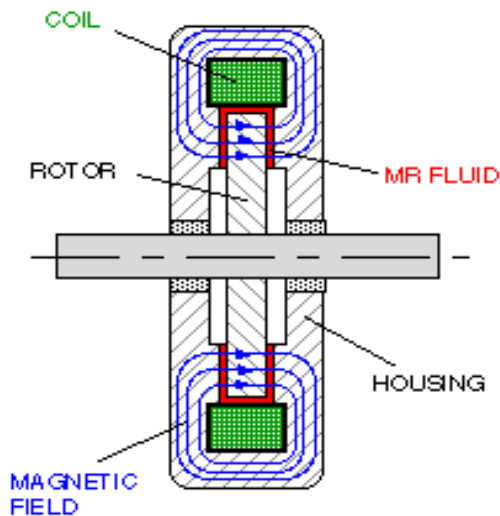


**FIG. 23. MRB-2107-3 Rotary Brake - Lord Corp.**

experimentally obtained plots of force versus velocity that display a hysteresis loop that does not pass through the origin (see FIG. 13). This indicates a deviation from the fundamental relationship between velocity and damping force that may be exploited in a creep resistant reverse MR damper. In addition, many widely accepted models for MR dampers such as the Bingham plastic model and the nonlinear viscoelastic-plastic model support an idealized creep resistant MR damper. The

Bingham plastic model assumes that the material will not flow and remains rigid in this pre-yield domain. The nonlinear viscoelastic-plastic model includes an equivalent stiffness term as part of its equation of motion for the viscoelastic portion of the damper force,  $f_{ve}$  (Pang *et al.*, 1998):

$$f_{ve}(t) = K_{ve}x(t) + C_{ve}\dot{x}(t) \quad (5)$$

where  $f_{ve}$  = viscoelastic damping force,  $K_{ve}$  = equivalent viscoelastic stiffness,  $C_{ve}$  = equivalent viscoelastic damping, and  $x$  = displacement. Equation 5 implies that even if the velocity of the damper is zero, the damper force is not required to also be zero.

Dejiana *et al.* (1997) present an MR damper as a “variable stiffness element” that possesses a critical resistance below which the damper behaves as a rigid body and the piston cannot move. They recommend that in order to incur a large force in a stiffness element, an MR damper with a bypass duct should be used. The longer the length of the duct and the smaller the thickness of the magnetized region of fluid, the more force the damper may sustain. These applications and theories coupled with the fact that much more research is necessary to fully explain the very structure of MR fluid emphasize that the answer to the creep question cannot yet be answered.

## **IX. DESIGN EXAMPLE OF A MAGNETORHEOLOGICAL DAMPER WITH REVERSE POWER REQUIREMENTS**

Although creep potential has caused the feasibility of a reverse MR damper to be in doubt, methods of power reversal still require discussion. The need to reverse the power requirements has been emphasized. Continuous solidification of MR fluid without the use of power may be accomplished through a permanent magnet. Softening of this damper may then be accomplished

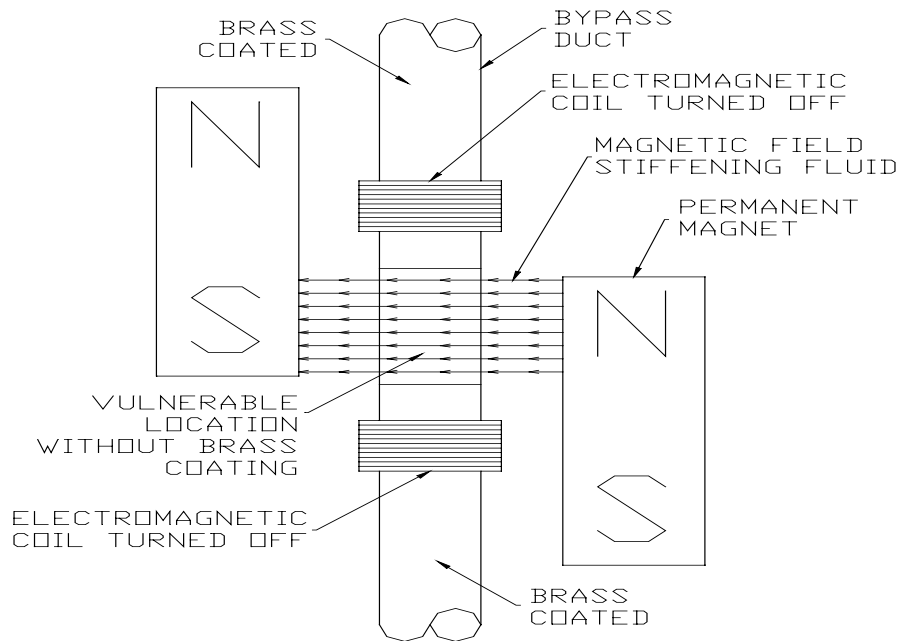


**FIG. 24. Example Reverse MR Damper Bypass Duct - "Locked" Position**

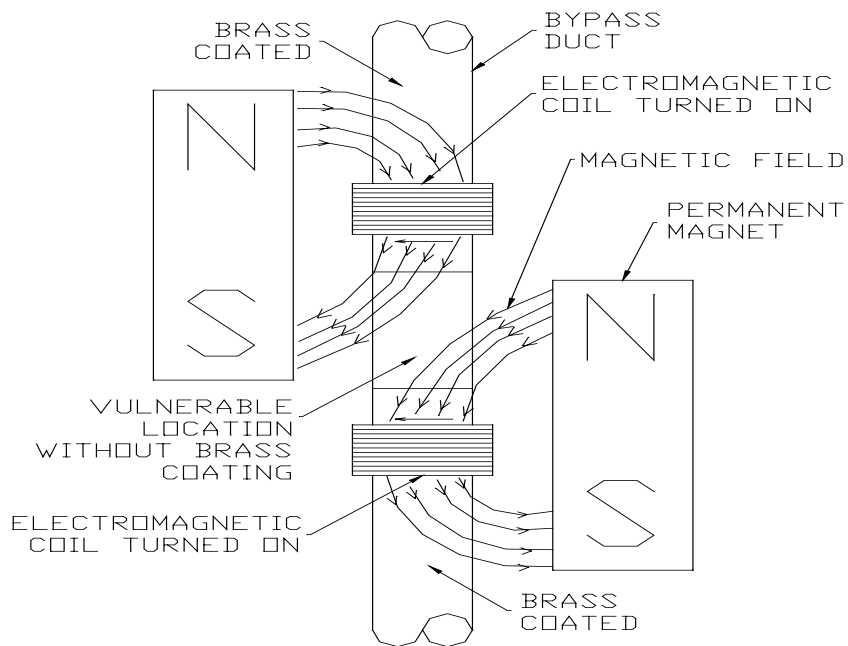


**FIG. 25. Example Reverse MR Damper Bypass Duct - "Unlocked" Position**

with an electromagnet positioned so that its field acts in the opposite direction of the field of the permanent magnet. Strengthening of the electromagnetic field, then, reduces the overall effective magnetic field magnitude and, thus, softens the MR damper.

One possible design elaborates on the design scheme for an MR damper that includes a bypass duct (see FIG. 17). The bypass duct may be coated with a substance possessing poor magnetic susceptibility, such as brass, that would protect the MR fluid inside from any magnetic field. One vulnerable location may be left unprotected allowing the north pole of a permanent magnet to be placed on one side of the location with the south pole of a different permanent magnet on the other side (see FIG. 24). This would provide a fully stiff MR damper without use of any power.

Softening the damper can be achieved with electromagnets located on either side of the vulnerable location on the bypass duct. FIG. 25 shows that each coil may be wound to produce an effective magnet that would serve as a complement of its neighboring permanent magnet. This would reroute the bulk of the magnetic field reducing the field through the duct and allowing the MR fluid to soften. Any excess magnetic field passing into the MR fluid would not be oriented perpendicular to the direction of intended fluid flow. Therefore, the particles would not be optimally aligned, and the residual magnetic field would have less effect on the fluid. Application of current to the coils softens the MR damper, and the power requirements have been reversed.

## **X. FUTURE RESEARCH AND CONCLUSIONS**

The above scheme is but one conceivable variation for the design of an MR damper with

reverse power requirements. The use of permanent magnets coupled with equivalent electromagnets appears to be a necessity in the design. Therefore, the critical factor controlling the design of MR dampers with reverse power requirements becomes the ability to resist creep. It is thus crucial to determine if an MR damper can be designed that fully resists creep. The rheological properties and capabilities of MR fluids must be fully explored and exploited in order to arrive at a creep resistant design. A deeper understanding of the fluid may lead to a better way of manipulating it for this purpose.

If creep of maximally stiffened MR dampers continues to plague their implementation, alternatives such as the use of variable orifice dampers exist for controlled deformation of critical truss members. Additionally, MR dampers with reverse power requirements that do not have to sustain a long-term static load may still be implemented in specific situations. These include circumstances where the surrounding elements of a truss system may not require the element containing the MR damper to maintain a significant long-term load. Another possible use arises for a truss system located in regions of the Earth's orbit where dead weight and long term sustained loads are negligible. Alternatively, these reverse MR dampers may be used to control structural vibration as some researchers are doing now with traditional MR dampers (Dejiang *et al.*, 1997).

Regardless of the discovery of a creep resistant design, currently available MR dampers should be tested to determine if they may be used to relieve the stress of a structural system as the numerical models have suggested. Strain and stress in a typical steel member for a defined displacement time history may be determined. The same displacement pattern can then be applied to a similar steel member with an MR damper installed along its axis. Strain and stress in the steel portion of the second test may be compared with the first to determine efficacy of the damper.

Corroboration of the numerical model in this way through actual experimentation may substantiate the feasibility of controlling deformation of critical truss members in order to prevent structural collapse during severe loading events.

Controlled deformation of critical truss members using MR dampers has been proven to be effective through numerical modeling that involves a control algorithm using fuzzy logic and a neural network. The stress level of a single degree of freedom truss element was maintained at a safe level when exposed to a simulated severe loading event. Concern for the physical implementation of an MR damper with reverse power requirements was addressed. The concepts of magnetorheological dampers with reverse power requirements and controlled deformation of critical truss members deserve more attention in future efforts toward advances in structural engineering.

## **XI. ACKNOWLEDGEMENTS**

The author would like to thank the Lord Corporation of Cary, North Carolina for use of a MRWD-002 light-duty magnetorheological damper. Prof. Paul N. Roschke has also earned sincere appreciation. He, Kyle Schurter, Mike Jones, Jin Zhang, and Byeonghwa Kim provided substantial aid and encouragement in this research endeavor.

## XII. REFERENCES

- Burton, S.A., Makris, N., Konstantopoulos, I., and Antsaklis, P.J. (1996). "Modeling the Response of ER Damper: Phenomenology and Emulation." *Journal of Engineering Mechanics*, Volume 122, Number 9, 897-906.
- Carlson, J.D., Catanzarite, D.N., and St. Clair, K.A. (1996). Commercial Magneto-Rheological Fluid Devices. *Proceedings 5th Int. Conf. on ER Fluids, MR Suspensions and Associated Technology*, Singapore, 20-28.
- Carlson, J.D., and Spencer, B.F. (1996). "Magneto-Rheological Fluid Dampers for Semi-Active Seismic Control." *Proceedings of the 3<sup>rd</sup> International Conference on Motion and Vibration Control*, Chiba, Japan, Volume III, 35-40.
- Dejiang, J., Jiaqi, C., and Jun, H. (1997). "Analysis and Design of Device of Electrorheological/ Magnetorheological Fluid with Variable Stiffness." *Proceedings of SPIE*, October 14-15, Pittsburgh, PA, USA, 204-212.
- Demuth, H., and Beale, M. (1997). *Neural Network Toolbox for Use with MATLAB: User's Guide*. Natick, MA: The MathWorks, Inc.
- Dyke, S.J., Spencer, B.F., Sain, M.K., and Carlson, J.D. (1996). "Experimental Verification of Semi-Active Control Strategies Using Acceleration Feedback." *Proceedings of the 3<sup>rd</sup> International Conference on Motion and Vibration Control*, Chiba, Japan, Volume III, 291-296.
- Dyke, S.J., Spencer, B.F., Sain, M.K., and Carlson, J.D. (1998). Modeling and Control of Magnetorheological Dampers for Seismic Response Reduction. *The University of Notre Dame's Structural Dynamics and Control/ Earthquake Engineering Laboratory Homepage*, [On-line]. [www.nd.edu/~quake/docs/research.htm](http://www.nd.edu/~quake/docs/research.htm).

- Jang, J.S.R., and Gulley, N. (1997). *MATLAB Fuzzy Logic Toolbox: User's Guide*. Natick, MA: The MathWorks, Inc.
- Jolly, M.R., Bender, B.W., and Carlson, J.D. (1998). Properties and Applications of Commercial Magnetorheological Fluids. *SPIE 5th Annual Int Symposium on Smart Structures and Materials*, San Diego, CA.
- Kordonsky, W.I., and Demchuk, S.A. (1996). Additional Magnetic Dispersed Phase Improves the MR-Fluid Properties. *Proceedings 5th International Conference on Electro-Rheological Fluids, Magneto-Rheological Suspensions and Associated Technology*, Singapore, 613-619.
- Lemaire, E., Bossis, G., and Volkova, O. (1996). Deformation and Rupture Mechanisms of ER and MR Fluids. *Proceedings 5th International Conference on Electro-Rheological Fluids, Magneto-Rheological Suspensions and Associated Technology*, Singapore, 368-375.
- Liu, J., Mou, T., Zhu, Y., Haddadian, E., Pousset, J., and Lim, S. (1996). Effects of Cell Confinement on the Evolution of Field-Induced Structures in a Magnetorheological Fluid. *Proceedings 5th International Conference on Electro-Rheological Fluids, Magneto-Rheological Suspensions and Associated Technology*, Singapore, 727-737.
- Makris, N., Burton, S.A., Hill, D., and Jordan, M. (1996). "Analysis and Design of ER Damper for Seismic Protection of Structures." *Journal of Engineering Mechanics*, Volume 122, Number 10, 1003-1011.
- Margida, A.J., Weiss, K.D., and Carlson, J.D. (1996). Magnetorheological Materials Based on Iron Alloy Particles. *Proceedings 5th International Conference on Electro-Rheological Fluids, Magneto-Rheological Suspensions and Associated Technology*, Singapore, 544-550.

*MRF-132LD Fluid* (1998). Product description and properties, [On-line].  
[www.rheonetic.com/mrfluid](http://www.rheonetic.com/mrfluid).

Pang, L., Kamath, G.M., and Wereley, N.M. (1998). “Analysis and Testing of a Linear Stroke Magnetorheological Damper.” *Proceedings of the 39<sup>th</sup> AIAA/ASME/ASCE/AHS/ASC Structures, Structural Dynamics, and Materials Conference and Exhibit and AIAA/ASME/AHS Adaptive Structures Forum*, Long Beach, CA, USA, Vol. 4, 2841-2856.

*Rheonetic Homepage*, [On-line]. (1998) [www.rheonetic.com/mrfluid](http://www.rheonetic.com/mrfluid).

Spencer, B.F., Carlson, J.D., Sain, M.K., and Yang, G. (1997). “On the Current Status of Magnetorheological Dampers: Seismic Protection of Full-Scale Structures.” *Proceedings of the 1997 American Control Conference*, Albuquerque, New Mexico, USA.

Spencer, B.F., Dyke, S.J., Sain, M.K., and Carlson, J.D. (1997). “Phenomenological Model For Magnetorheological Dampers.” *ASCE Journal of Engineering Mechanics*, Volume 123, No. 3, 230-238.

Soong, T.T. (1990). *Active Structural Control: Theory and Practice*. Essex, England: Longman Scientific and Technical.

Tang, X., Chen, Y., and Conrad, H. (1996). Structure and Interaction Force in a Model Magnetorheological System. *Proceedings 5th International Conference on Electro-Rheological Fluids, Magneto-Rheological Suspensions and Associated Technology*, Singapore, 603-612.

Zhang, J. and Roschke, P.N., (1998). “Neural Network Simulation of Magnetorheological Damper Behavior.” *Proceedings of the International Conference on Vibration Engineering '98*, Dalian, China.

### **XIII. BIBLIOGRAPHY**

- Buchholdt, H.A. (1997). *Structural Dynamics for Engineers*. London: Thomas Telford Publications.
- Doyle, J.F. (1991). *Static and Dynamic Analysis of Structures with an Emphasis on Mechanics and Computer Matrix Methods*. Dordrecht, The Netherlands: Kluwer Academic Publishers.
- Dyke, S.J., Spencer Jr., B.F., Quast, P., Sain, M.K., Kaspari Jr., D.C., and Soong, T.T. (1996, September). "Acceleration Feedback Control of MDOF Structures." *Journal of Engineering Mechanics*, 907-917.
- Felt, D.W., Hagenbuchle, M., Liu, J., and Richard, J. (1996). Rheology of a Magnetorheological Fluid. *Proceedings 5th International Conference on Electro-Rheological Fluids, Magneto-Rheological Suspensions and Associated Technology*, Singapore, 738-746.
- Furuta, H., Kawakami, S., Kaneyoshi, M., and Tanaka, H. (1995). Practical Application of Fuzzy Tension Adjustment to Bridge Construction. *Restructuring: America and Beyond, ASCE Conference Proceedings*, New York, 1651-1654.
- Ginder, J.M., Davis, L.C., and Elie, L.D. (1996). Rheology of Magnetorheological Fluids: Models and Measurements. *Proceedings 5th International Conference on Electro-Rheological Fluids, Magneto-Rheological Suspensions and Associated Technology*, Singapore, 504-514.
- Hagenbuchle, M., Sheaffer, P., Zhu, Y., and Liu, J. (1996). Static and Dynamic Light Scattering of Dilute Magnetorheological Emulsions. *Proceedings 5th International Conference on Electro-Rheological Fluids, Magneto-Rheological Suspensions and Associated Technology*, Singapore, 236-244.

Hanselman, D., and Littlefield, B. (1996). *Mastering MATLAB: A Comprehensive Tutorial and Reference*. Upper Saddle River, New Jersey: Prentice-Hall.

Jones, H. (1998). “CVEN 445: Matrix Structural Analysis.” *Class Notes*. College Station, Texas. Texas A&M University.

Koyama, K. (1996). Rheological Synergistic Effects of Electric and Magnetic Fields in Iron Particle Suspension. *Proceedings 5th International Conference on Electro-Rheological Fluids, Magneto-Rheological Suspensions and Associated Technology*, Singapore, 245-250.

*MATLAB High-Performance Numeric Computation and Visualization Software: Reference Guide*. (1994). Natick, Massachusetts: The MathWorks, Inc.

Miyamoto, H.K., and Scholl, R.E. (1998, November). Steel Pyramid. *Modern Steel Construction*, 42-48.

Oregon Hospital Braces for Natural Disaster. (1998, December). *Civil Engineering*, 26-27.

Smart Fluid Dampens Seismic Forces. (1998, December). *Civil Engineering*, 27.

Young, H.D., and Freedman, R.A. (1996). *University Physics, Ninth Edition*. Reading, Massachusetts: Addison-Wesley Publishing Company.

## XIV. APPENDIX

### A. COMPUTER CODE

A list of the major components of the MATLAB, Simulink, fuzzy control, and neural network code is given below. Each component is shown either graphically or as source code and is presented in order of use.

- I. ***trussinit.m*** – MATLAB m-file that initializes the Simulink model of MR damper behavior
- II. ***trussimbackup.mdl*** – Overall Simulink model prior to installation of the neural network providing current information
- III. ***Control Algorithm*** – Simulink subsystem of *trussimbackup.mdl* that uses a Fuzzy Inference System to determine a modified damping and stiffness factor
- IV. ***mrstiff.m*** – MATLAB m-file that trained the neural network used in the Simulink model
- V. ***trussim.mdl*** – Overall Simulink model including the neural network providing current information
- VI. ***Control Algorithm*** – Simulink subsystem of *trussim.mdl* that uses a Fuzzy Inference System to determine a stiffness factor
- VII. ***Input of Initial Constants: Ko, Co, M*** – Simulink subsystem shared by *trussimbackup.mdl* and *trussim.mdl* that assigns the initial values of stiffness, damping, and mass for the truss
- VIII. ***Displacement Generator*** - The Simulink subsystem shared by *trussimbackup.mdl* and *trussim.mdl* that generates the semi-random displacement that serves as the input for the model
- IX. ***Differentiate...*** - Simulink subsystem shared by *trussimbackup.mdl* and *trussim.mdl* that differentiates the input displacement to obtain velocity and acceleration

- X. ***Determine Uncontrolled Stress*** - Simulink subsystem shared by *trussbackup.mdl* and *trussim.mdl* that determines the uncontrolled stress based upon initial constants, displacement, velocity, and acceleration
- XI. ***Fuzzy Inference System*** - Simulink subsystem shared by *trussbackup.mdl* and *trussim.mdl* that provides *percent of stiffening capacity* based upon stress feedback
- XII. ***Determine Controlled Stress*** - Simulink subsystem shared by *trussbackup.mdl* and *trussim.mdl* that determines the controlled stress based upon the mass, damping, modified stiffness, displacement, velocity, and acceleration
- XIII. ***Plot...*** - Simulink subsystem shared by *trussbackup.mdl* and *trussim.mdl* that produces the final plot of controlled and uncontrolled stress
- XIV. ***FIS General Editor*** – Main graphical menu for the Fuzzy Inference System used in *trussbackup.mdl* and *trussim.mdl*
- XV. ***FIS Rule Editor*** – Graphical interface used to establish the rules that govern the Fuzzy Inference System used in *trussbackup.mdl* and *trussim.mdl*
- XVI. ***FIS Input Membership Function Editor*** - Graphical interface used to establish the input membership functions for the Fuzzy Inference System used in *trussbackup.mdl* and *trussim.mdl*
- XVII. ***FIS Output Membership Function Editor*** - Graphical interface used to establish the output membership functions for the Fuzzy Inference System used in *trussbackup.mdl* and *trussim.mdl*

## I. *trussinit.m*

```
% Initialization for truss simulation

%      Filename:  trussinit.m

adjustedtrussfis = readfis('adjustedtrussfis.fis') ;

YieldStress = 1000

Ko = 1000    %Stiffness
Co = 10      %Damping Coefficient
M = 10       %Mass
Area = 1     %Cross-Sectional Area

PercentStiff = 100;    %Initial Percent of Stiffening Capacity

MinPercentStiff = 17.87

displacementamp = 1.25

%Weights and Biases for the Neural Network:

w1 = [0.4597
      0.1039
      0.0446
      -0.4478
      -0.1938]

b1 = [-0.3411
      -20.4897
      -2.4054
      -3.5194
      20.7210]

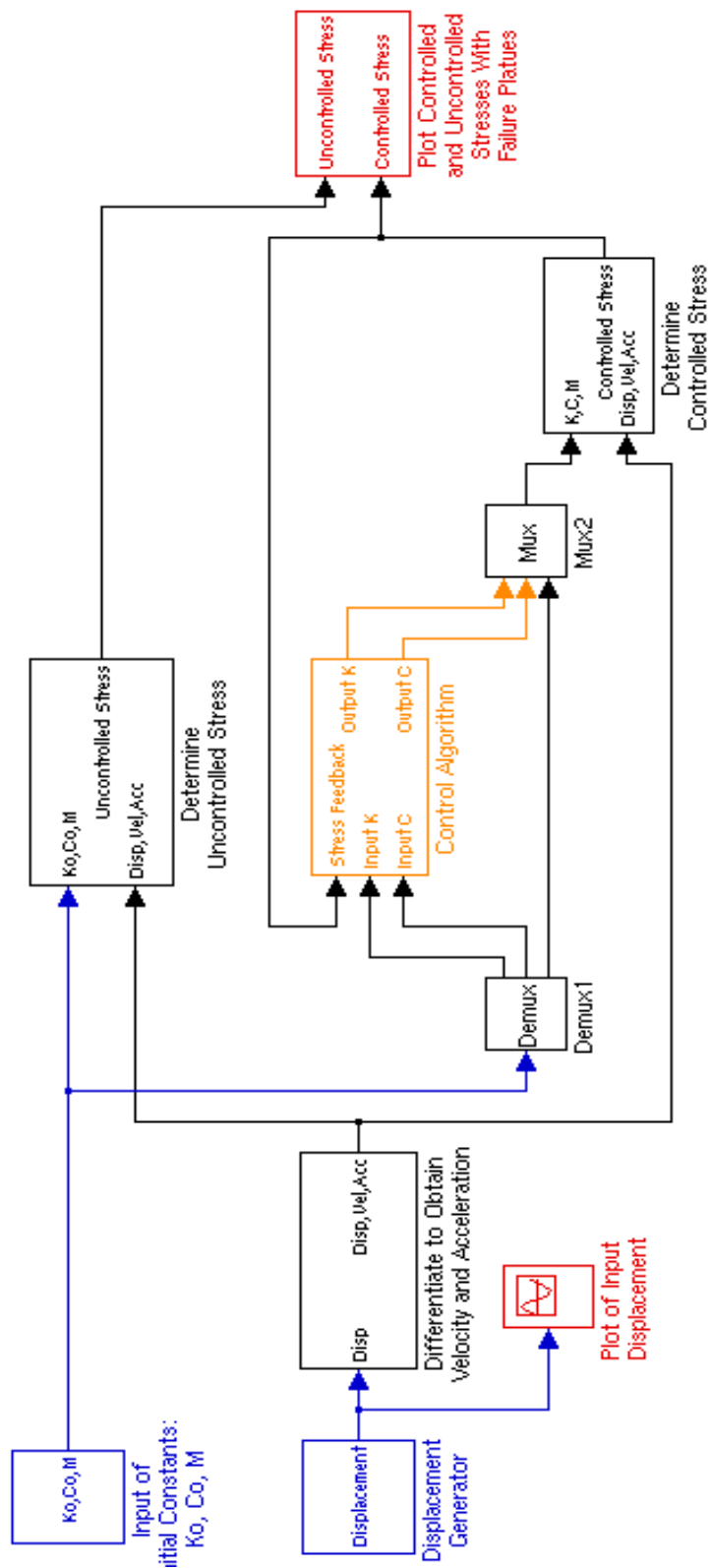
w2 = [-0.0264 -1.2026 0.4207 -0.2152 -1.7986]

b2 = [0.7955]

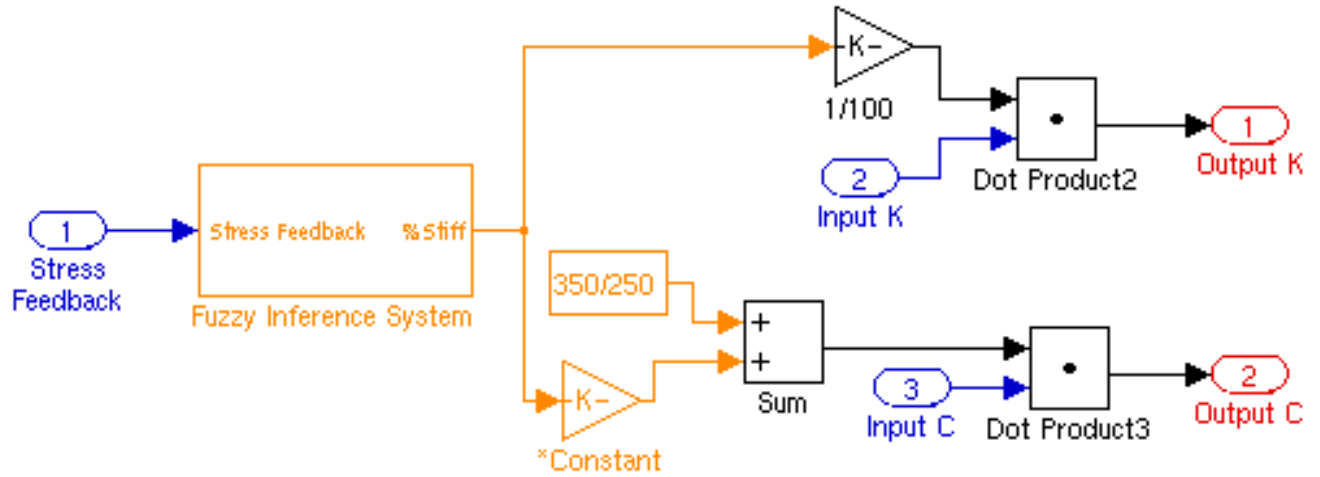
%      Start the fuzzy simulation

trussim.mdl
```

## II. *trussimbackup.mdl*



### III. Control Algorithm



#### IV. *mrstiff.m*

```
echo on

% This is a
%   SINGLE INPUT/ SINGLE OUTPUT
%   routine that uses a neural network to provide a value of
current
%   necessary to provide an MR damper depending on the desired
%   input stiffness of the damper.

% define input vector:      (K=stiffness)

K=[0.0 17.87 38.90 42.95 48.81 54.62 61.45 66.16 80.48 90.04 98.68
100.00]

% define targets for these inputs:      (A=current)

A=[0.0 0.0 0.1 0.2 0.3 0.4 0.5 0.6 0.7 0.8 0.9 1.0]

%plot the points

figure(1)
plot(A,K,'+')
title('Training Vectors')
ylabel('Input Vector K = Stiffness')
xlabel('Target Vector A = Current')

% design a 2-layer TANSIG/PURELIN network
% First, set the number of TANSIG neurons in the hidden layer:

S1 = 5

% INITFF is used to initialize the weights and biases
% for the TANSIG/PURELIN network

[w1,b1,w2,b2] = initff(K,S1,'logsig',A,'purelin')

% Training the network
% TRAINBP uses backpropagation to train feed-forward networks.
% TRAINBPX and TRAINLM are other choices that MAY be faster.

df = 20      %Frequency of progress displays (in epochs)
me = 2000    %Maximum number of epochs to train
eg = 0.0075  %Sum-squared error goal
```

```

lr = 0.01      %Learning rate

tp = [df me eg lr];

% Training begins:

[w1,b1,w2,b2,ep,tr] =
trainlm(w1,b1,'tansig',w2,b2,'purelin',K,A,tp);

% Testing the network:

trial = 0:100;

result = simuff(trial,w1,b1,'tansig',w2,b2,'purelin');

figure(2);
plot(A,K,'+',result,trial,'m');
title('Testing the Network');
ylabel('Input Vector K = Stiffness')
xlabel('Target Vector A = Current')

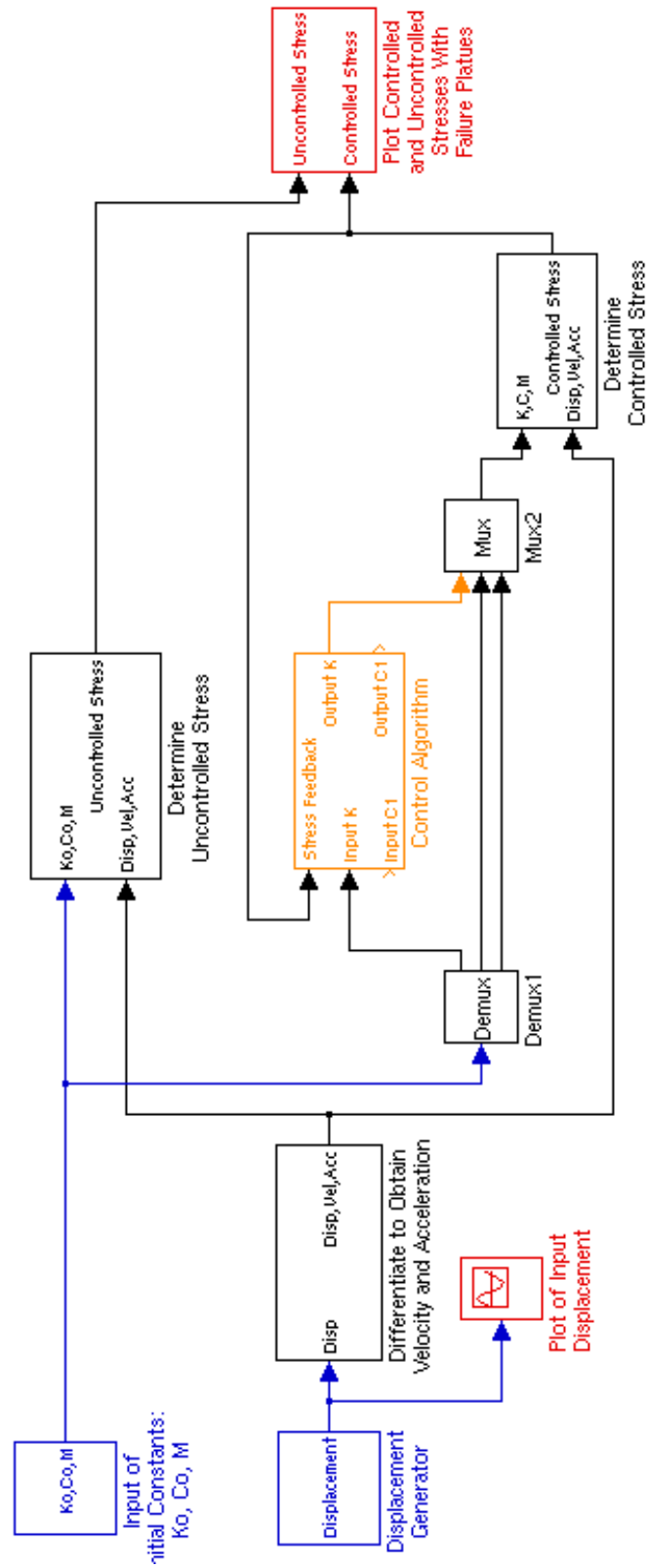
% changing the error goal (eg) should result in a closer
approximation.

%neuralsimulink

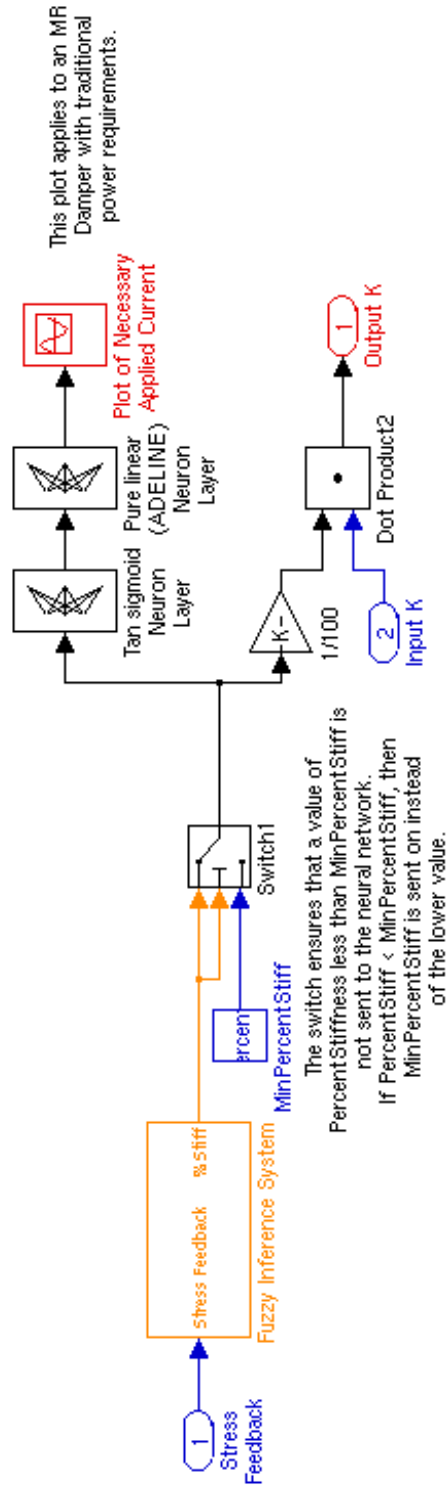
echo off;
return

```

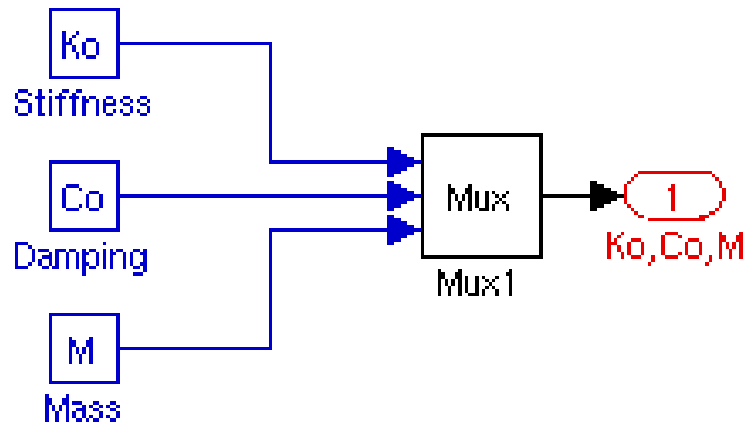
V. *trussim.mdl*



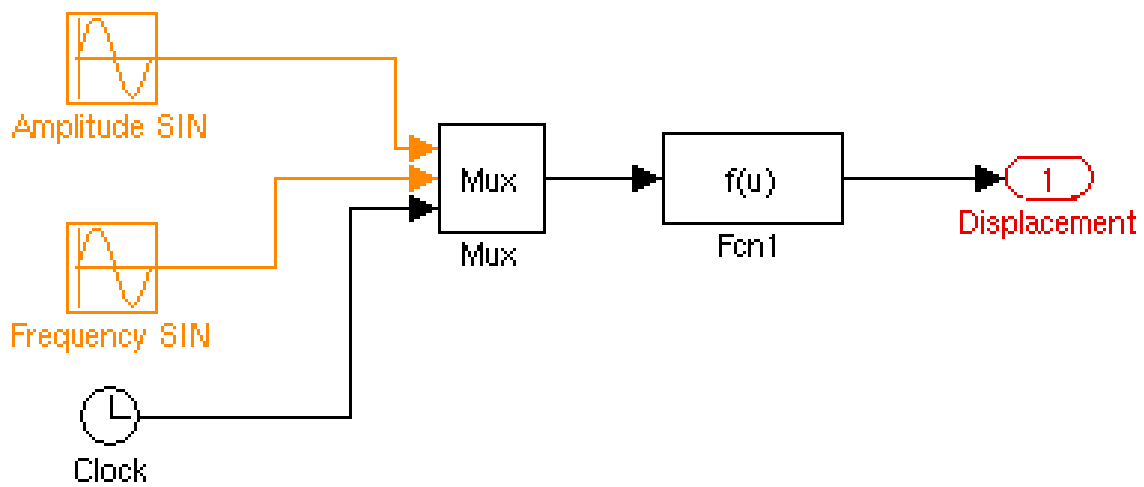
## VI. Control Algorithm



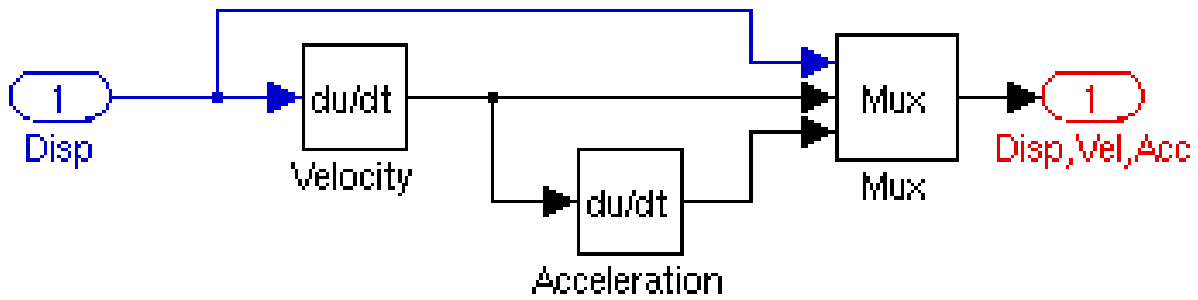
## VII. *Input of Initial Constants: $K_o$ , $C_o$ , $M$*



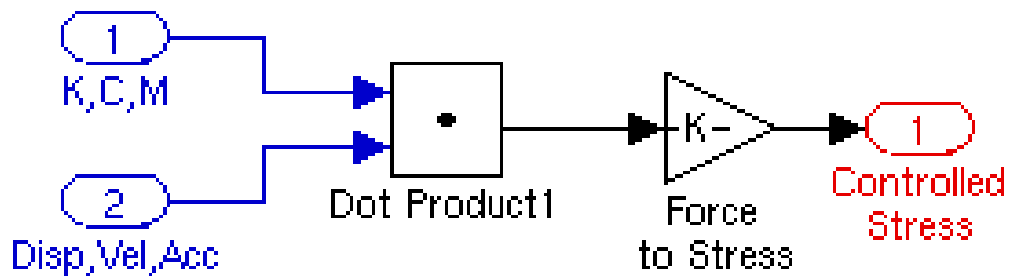
## VIII. *Displacement Generator*



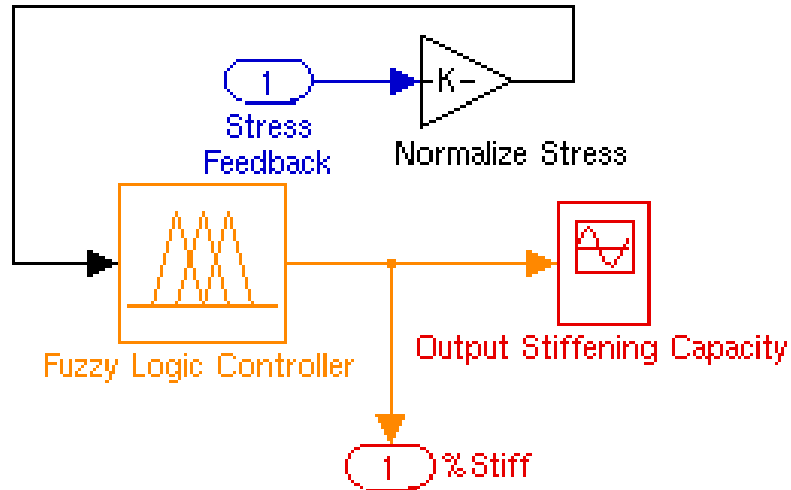
IX. *Differentiate to Obtain Velocity and Acceleration*



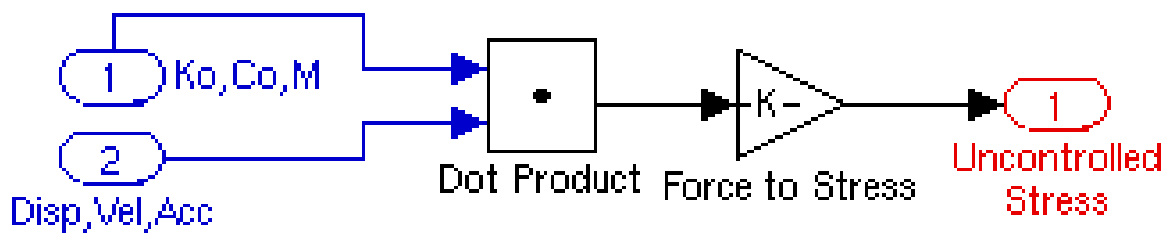
X. *Determine Uncontrolled Stress*



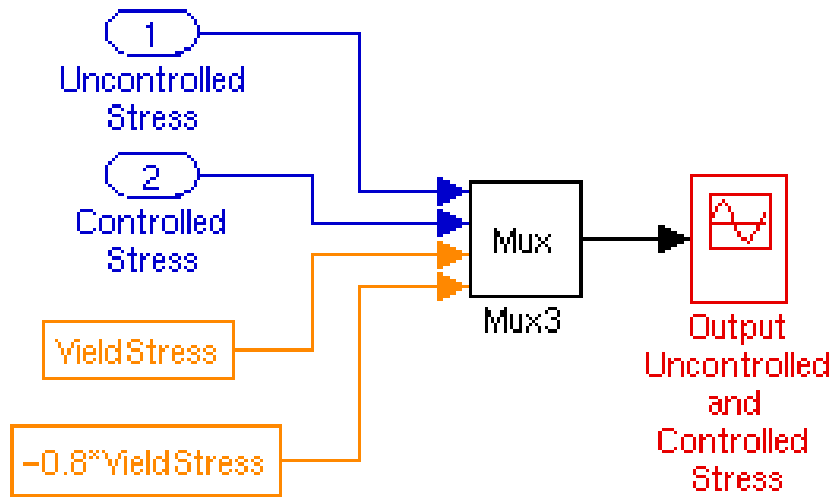
## XI. Fuzzy Inference System



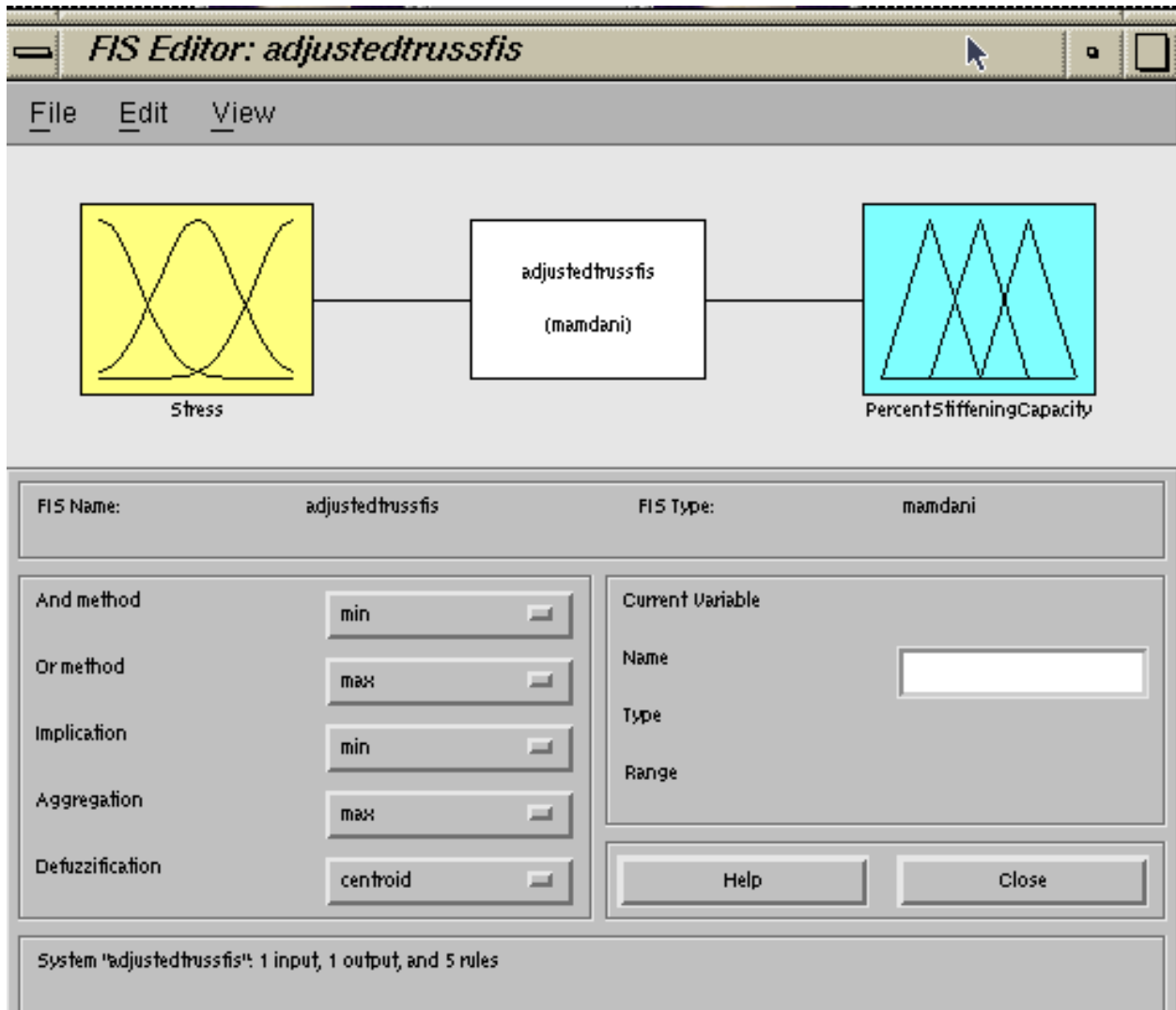
## XII. Determine Controlled Stress



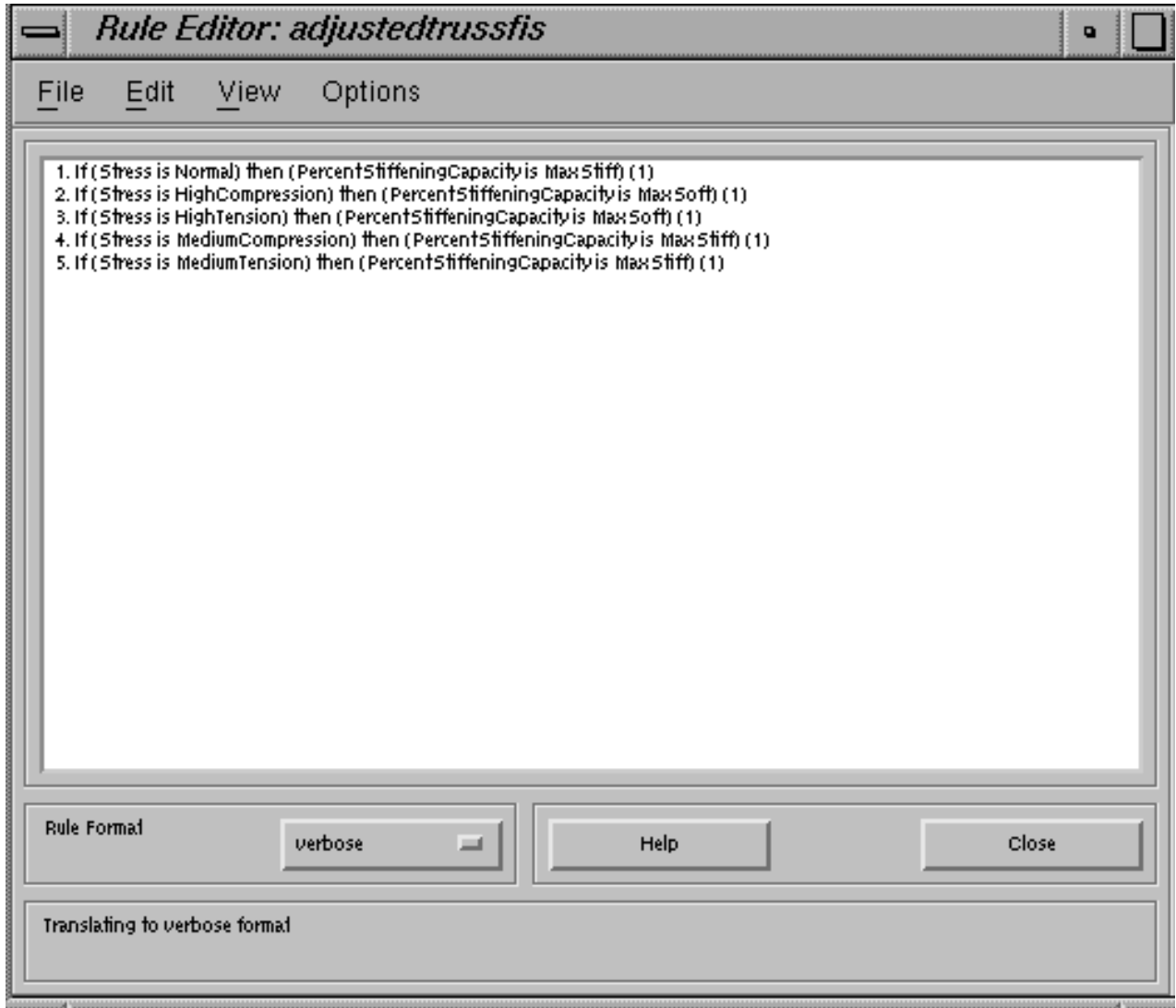
XIII. *Plot Controlled and Uncontrolled Stress with Failure Plateaus*



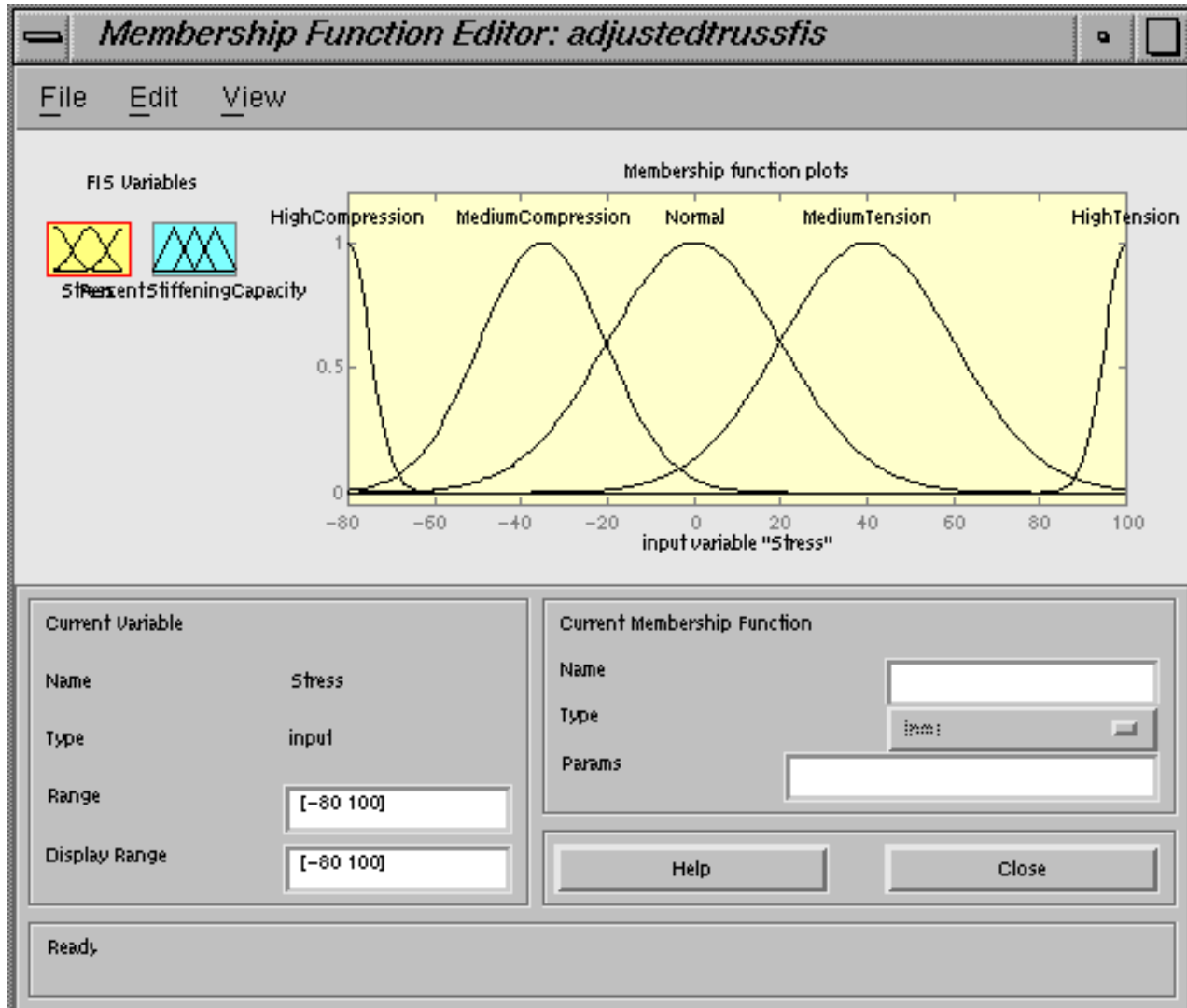
#### XIV. FIS General Editor



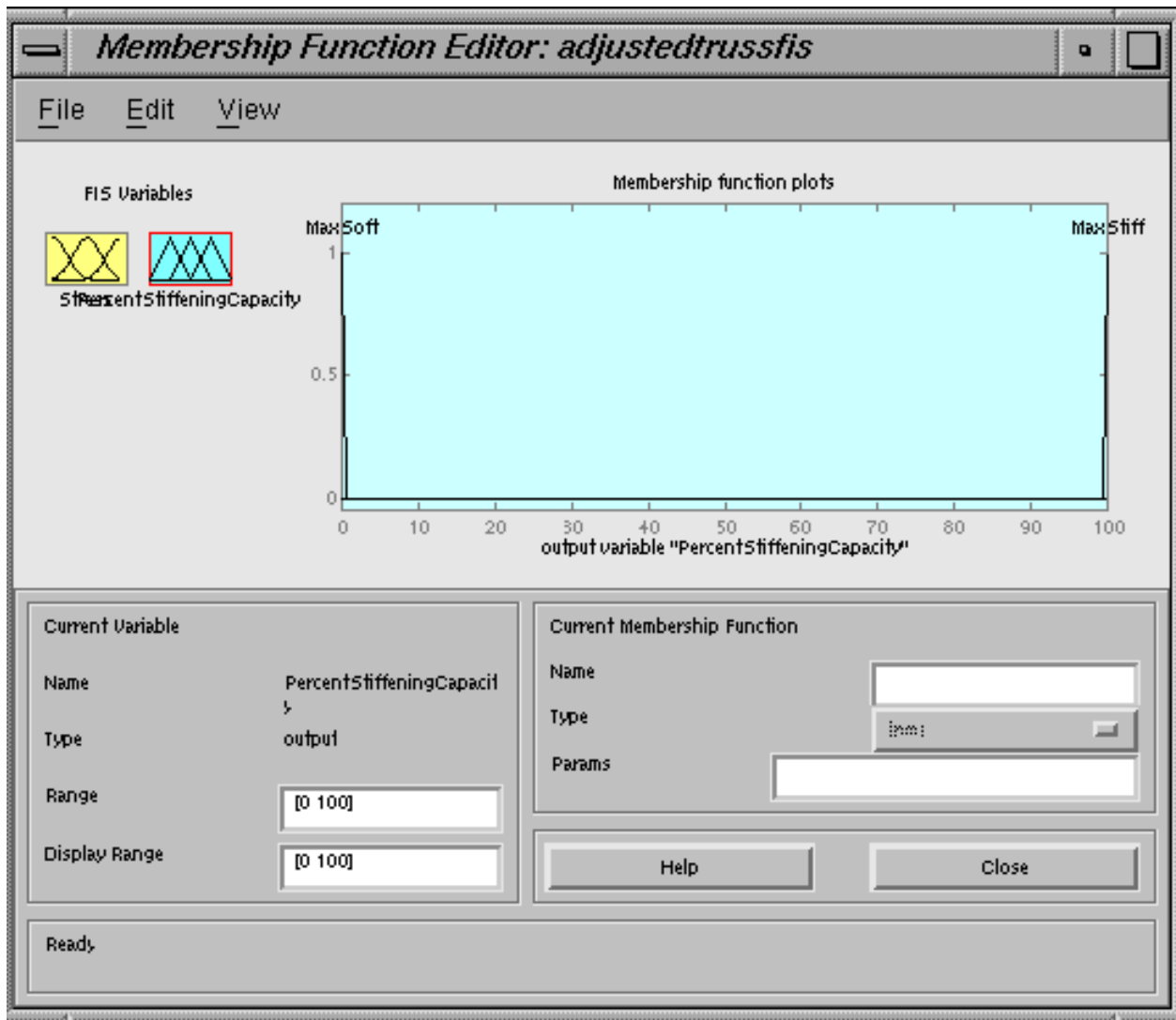
## XV. FIS Rule Editor



## XVI. FIS Input Membership Function Editor



## XVII. FIS Output Membership Function Editor



## B. EXPERIMENTAL PLOTS

For each of the levels of applied current to the magnetorheological damper (see TABLE 1), the following plots of displacement versus force and velocity versus force were created. Notice that they are all plotted to the same scale so that the effect of decreasing magnetic field is obvious.

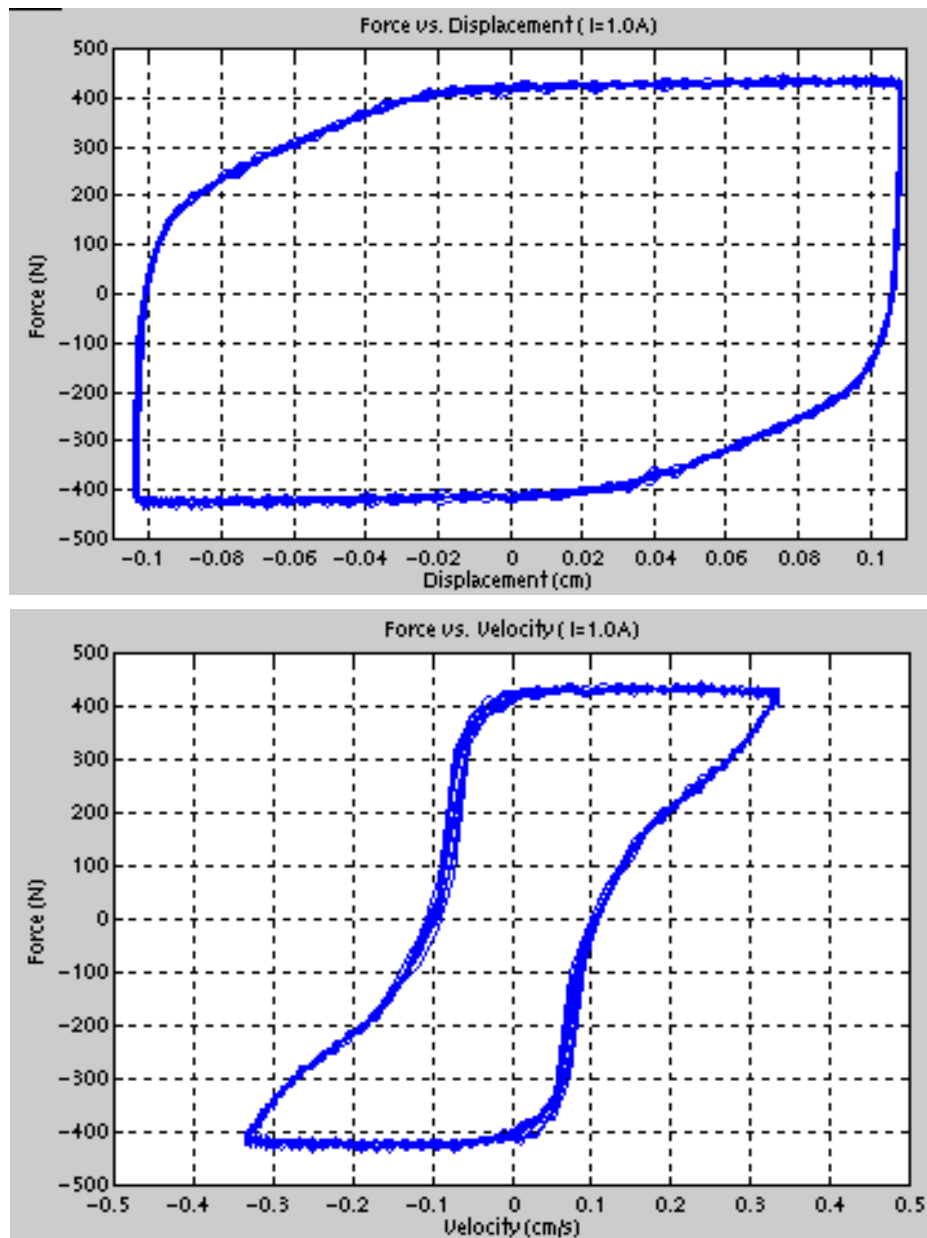


**FIG. B-1. Current = 1.0 amps**

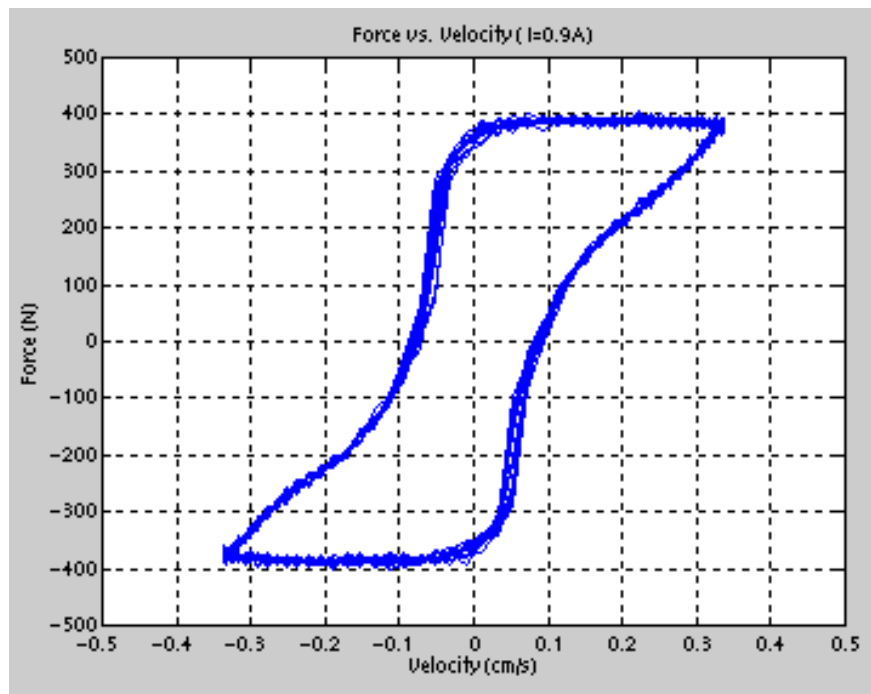
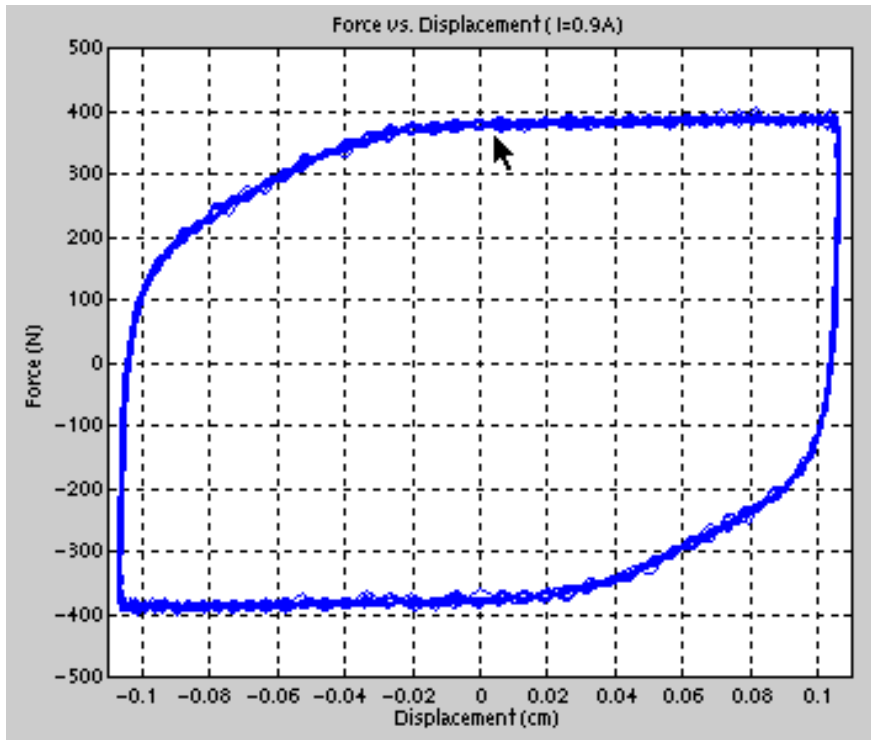


**FIG. B-2. Current = 0.9 amps**

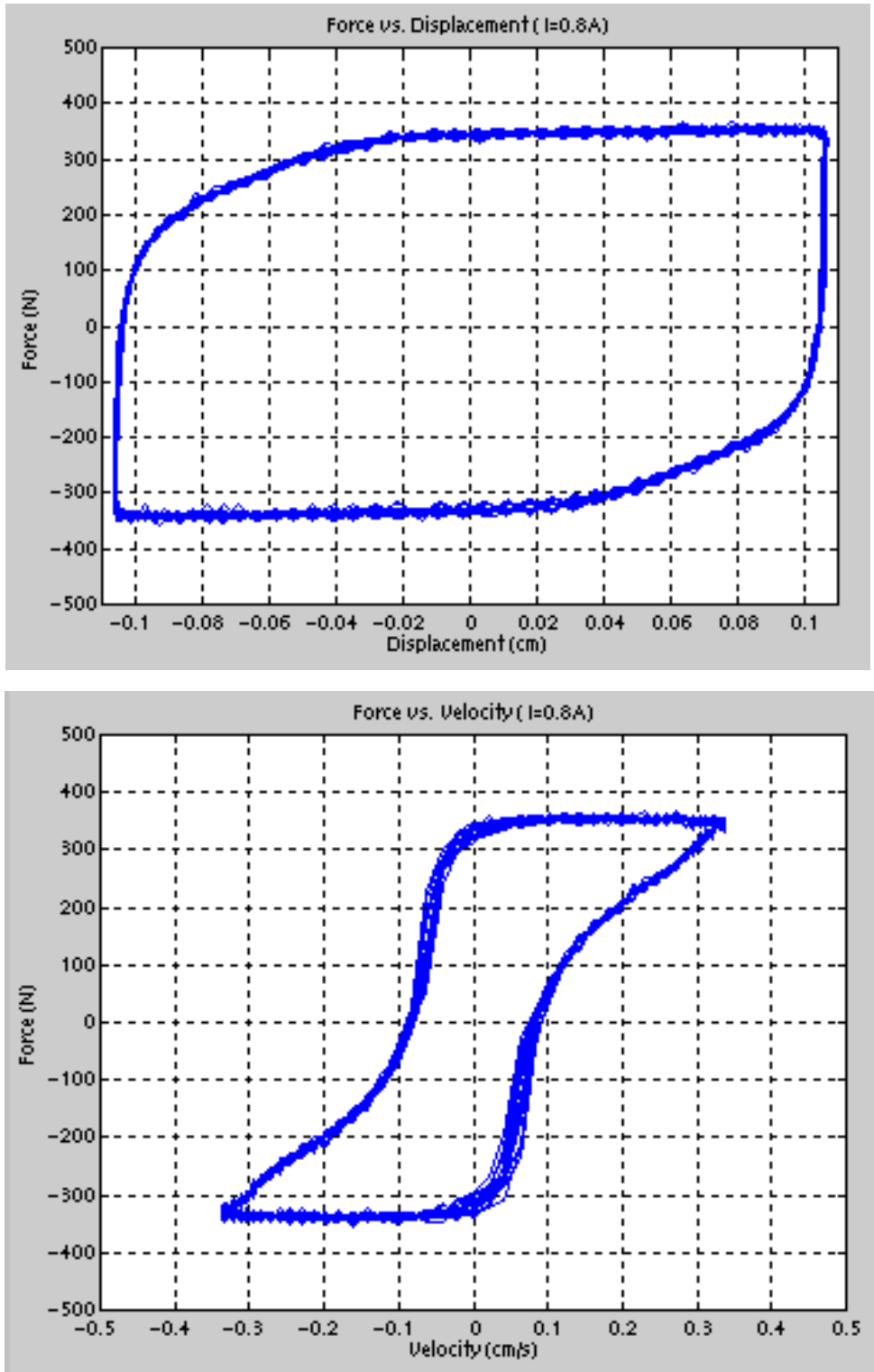


FIG. B-3. Current = 0.8 amps

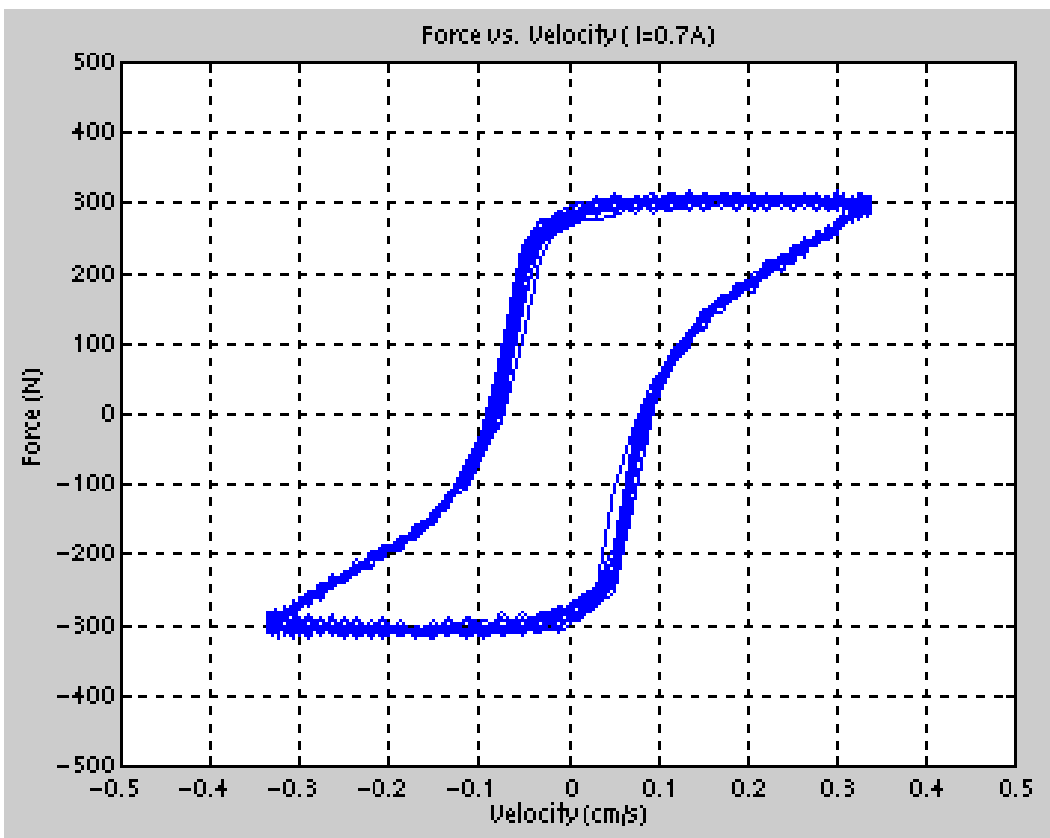
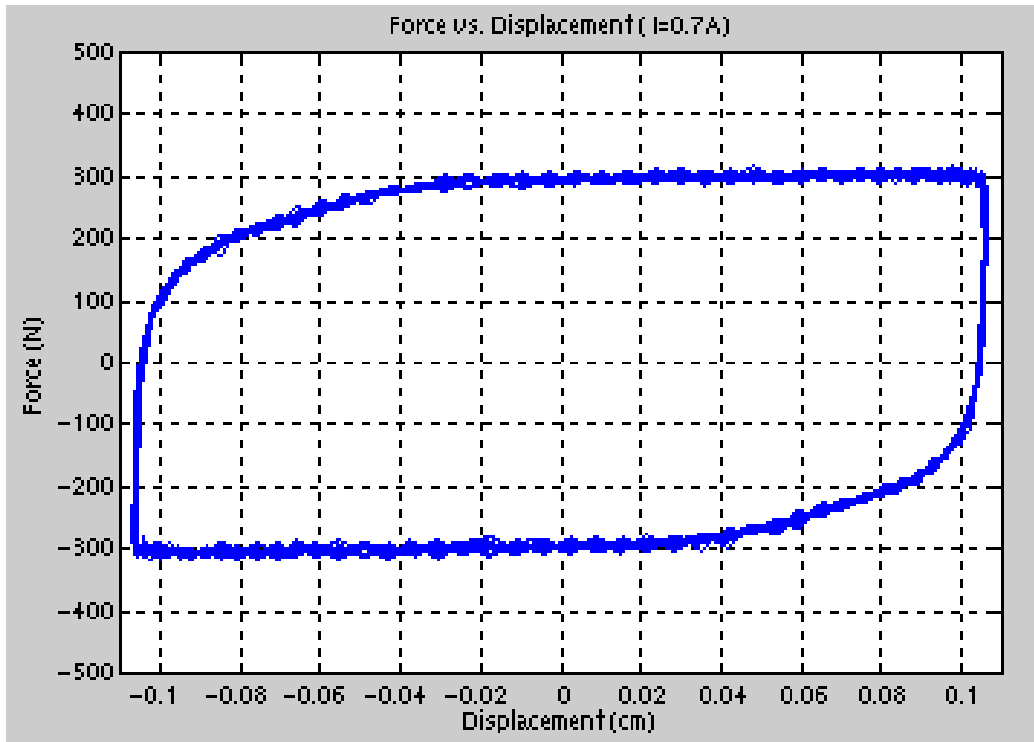


FIG. B-4. Current = 0.7

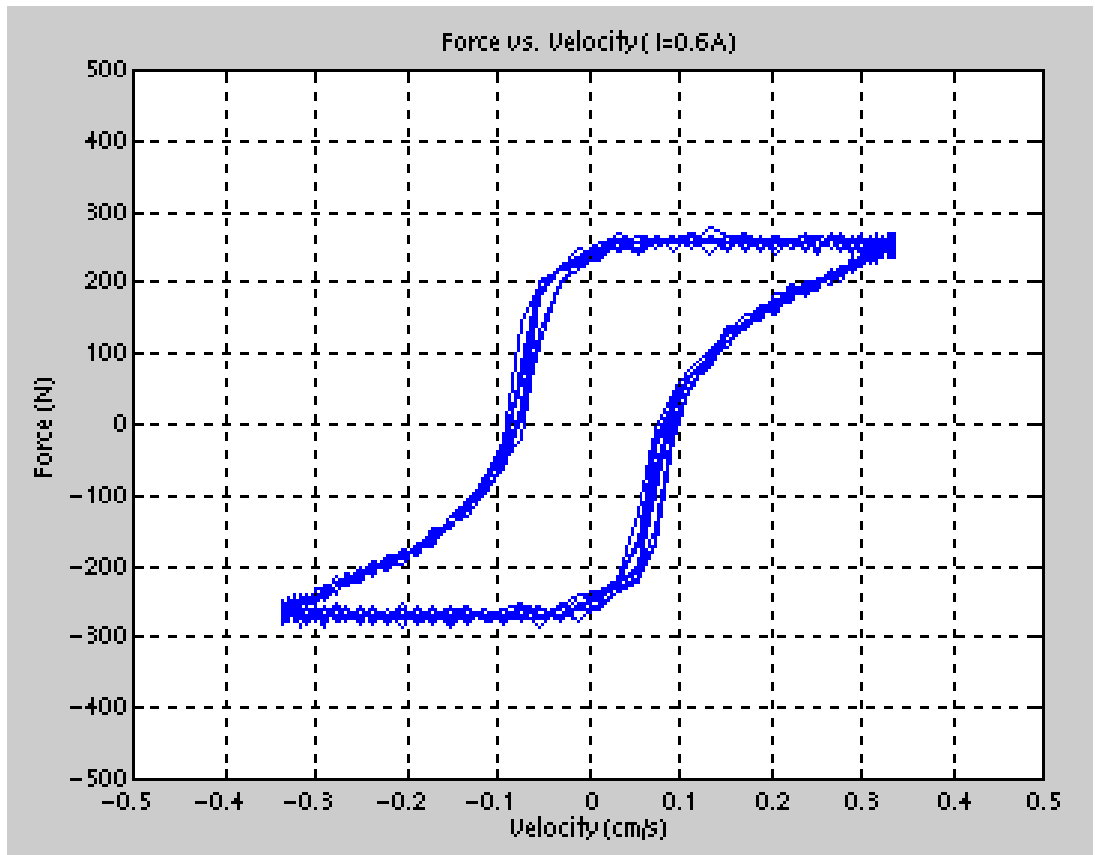
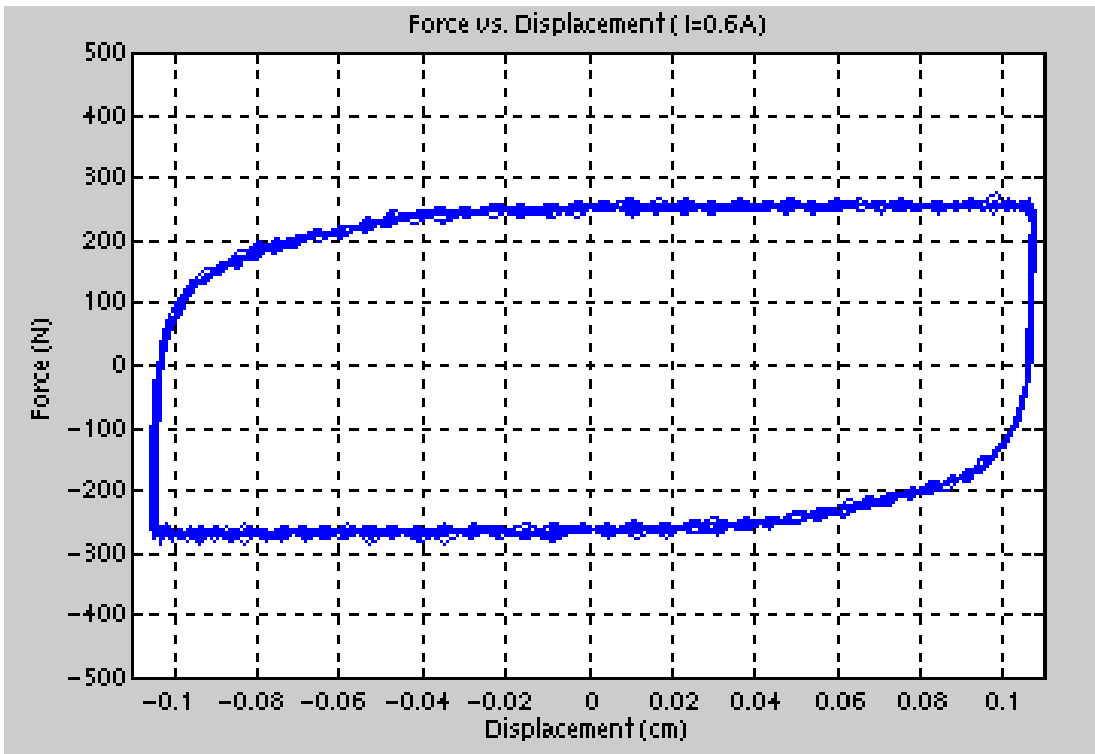
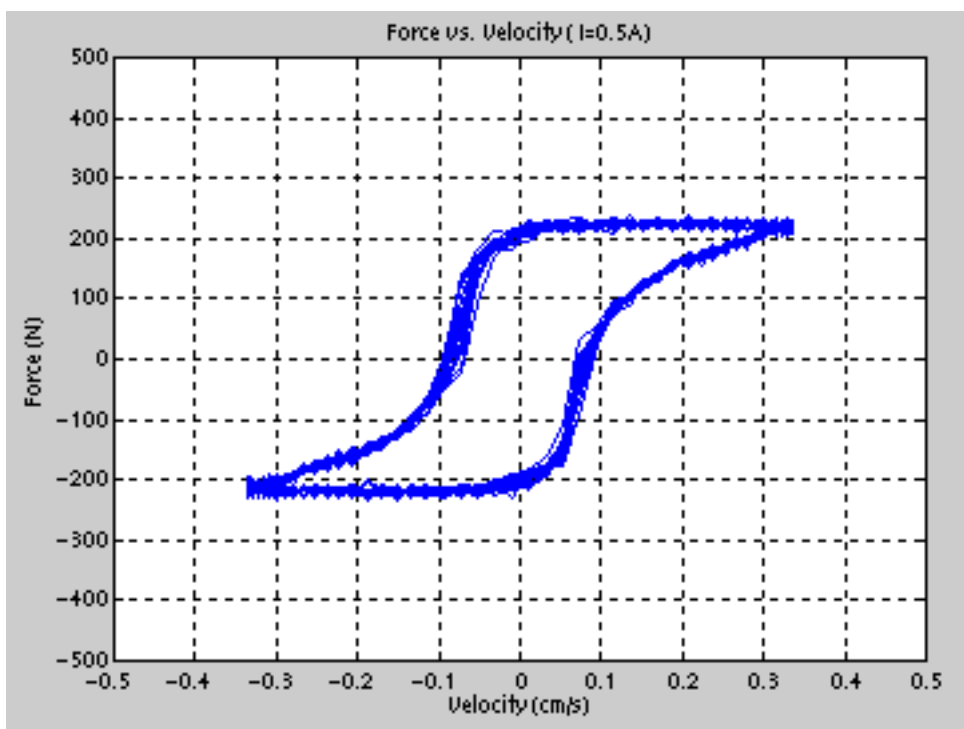
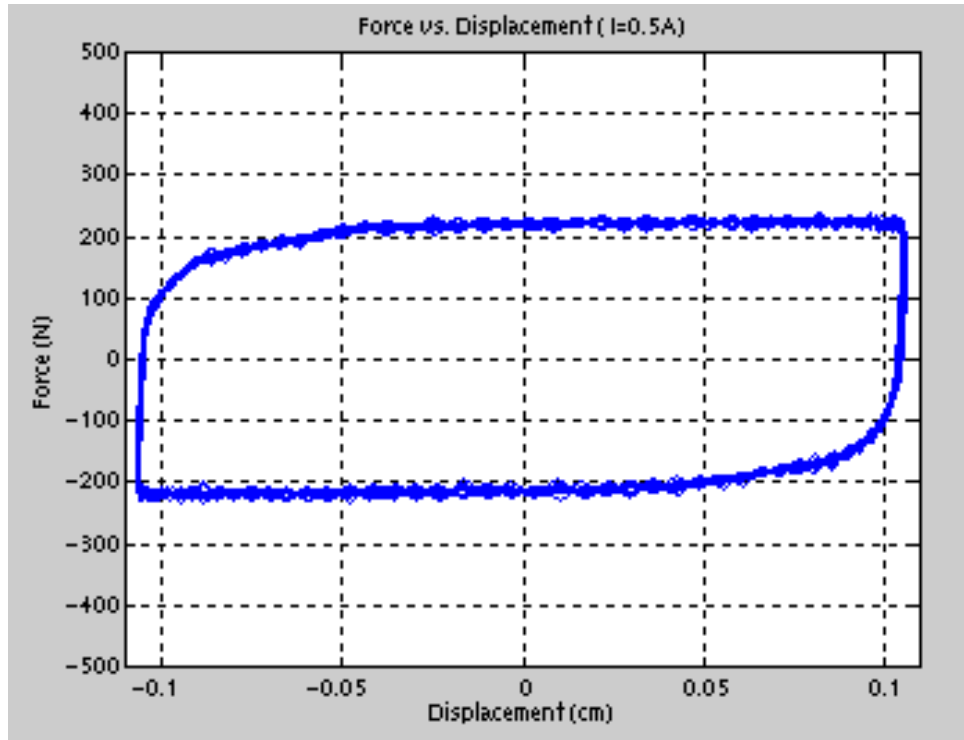
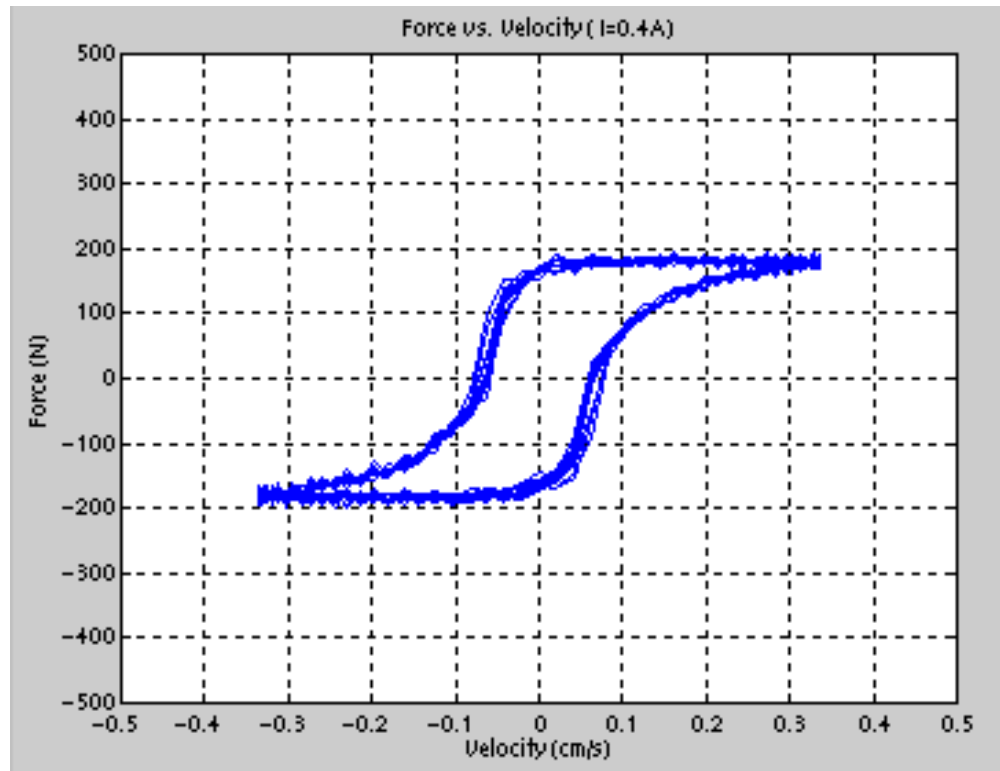
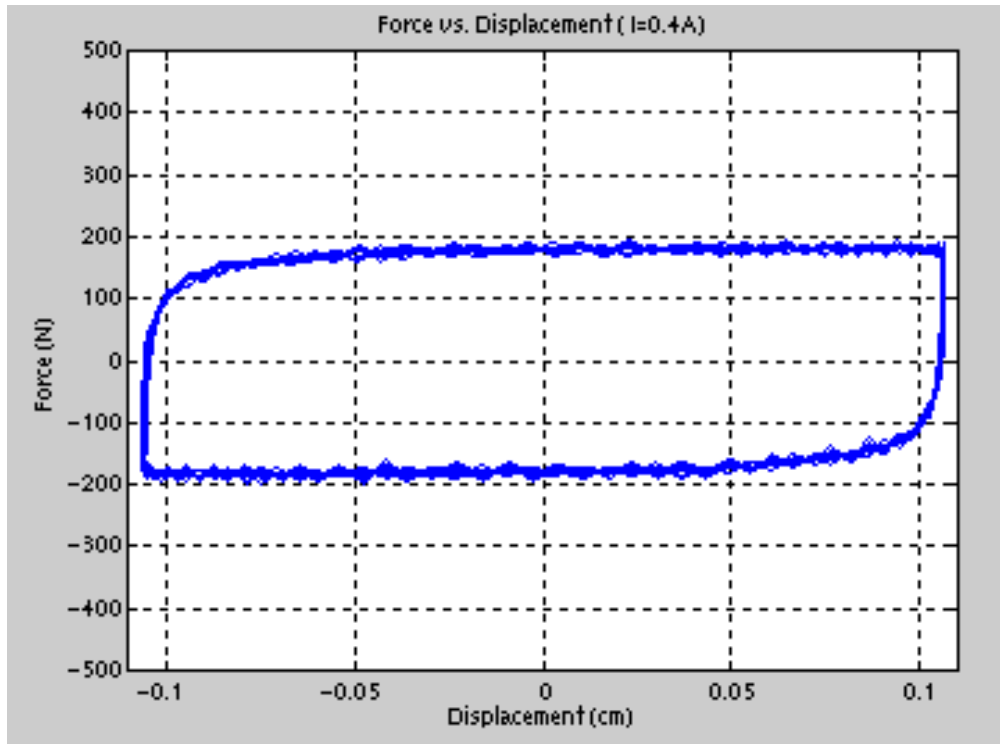


FIG. B-5. Current = 0.6 amps



**FIG. B-6. Current = 0.5 amps**



**FIG. B-7. Current = 0.4 amps**

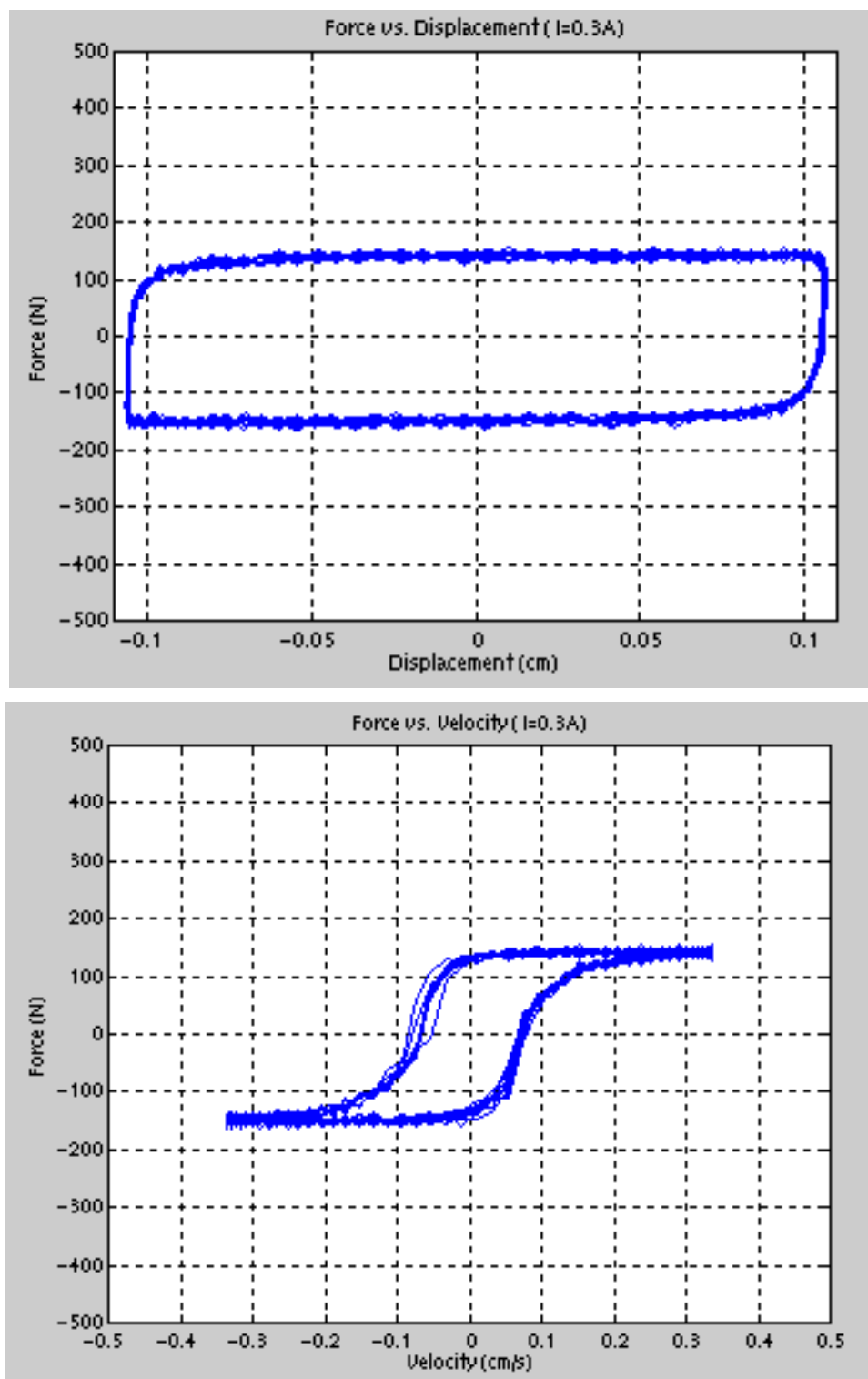


**FIG. B-8. Current = 0.3 amps**

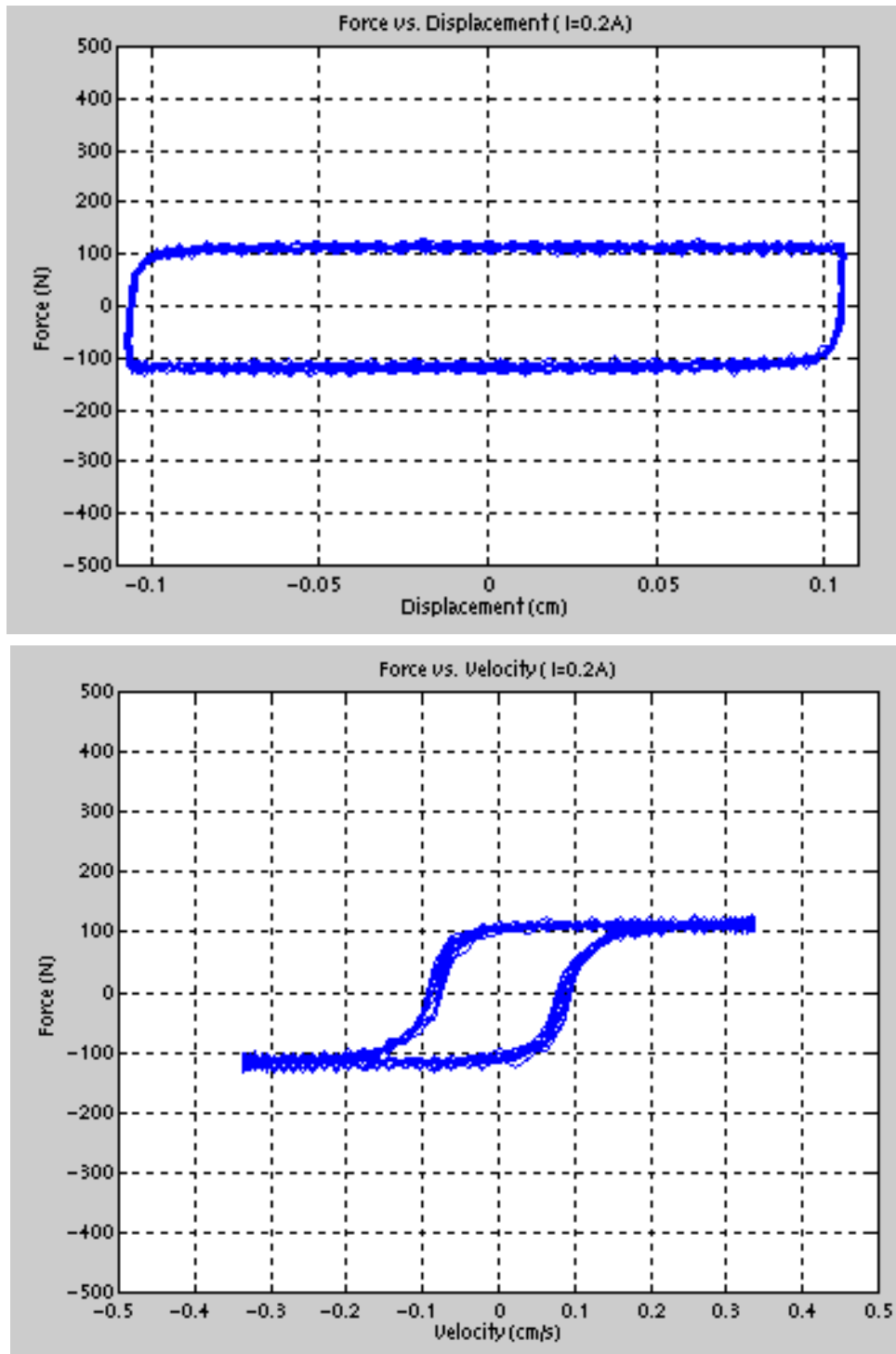


**FIG. B-9. Current = 0.2 amps**

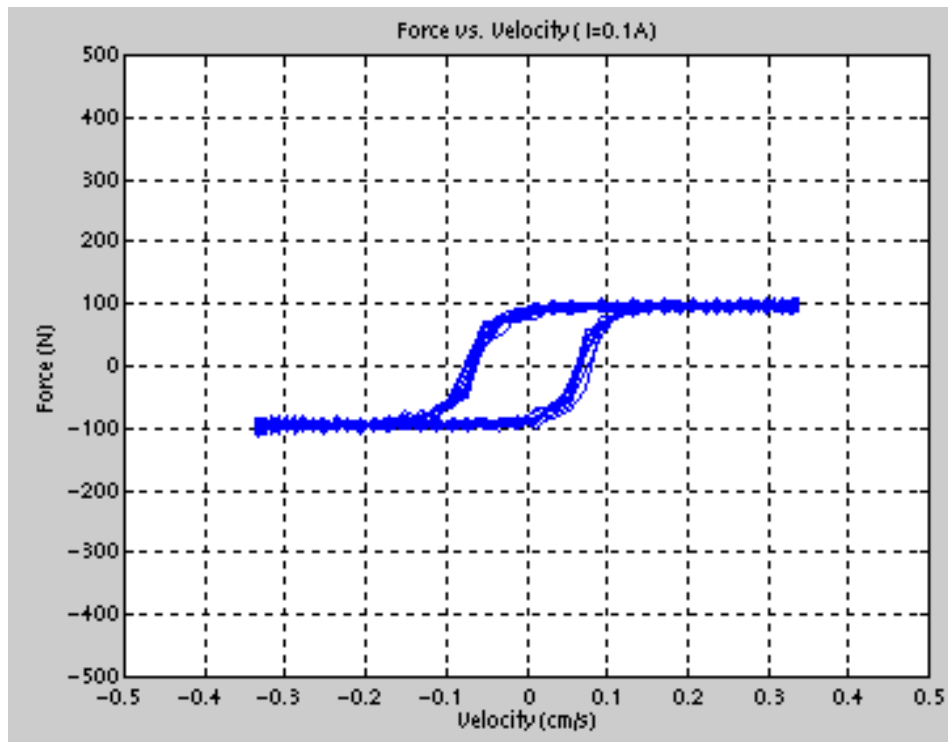
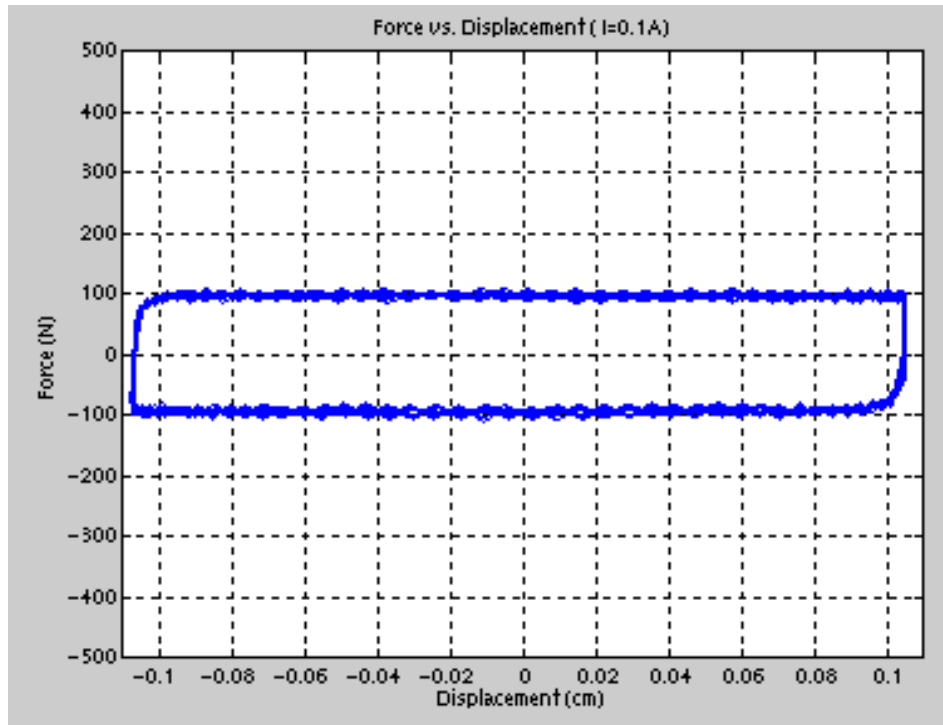


**FIG B-10. Current = 0.1 amps**

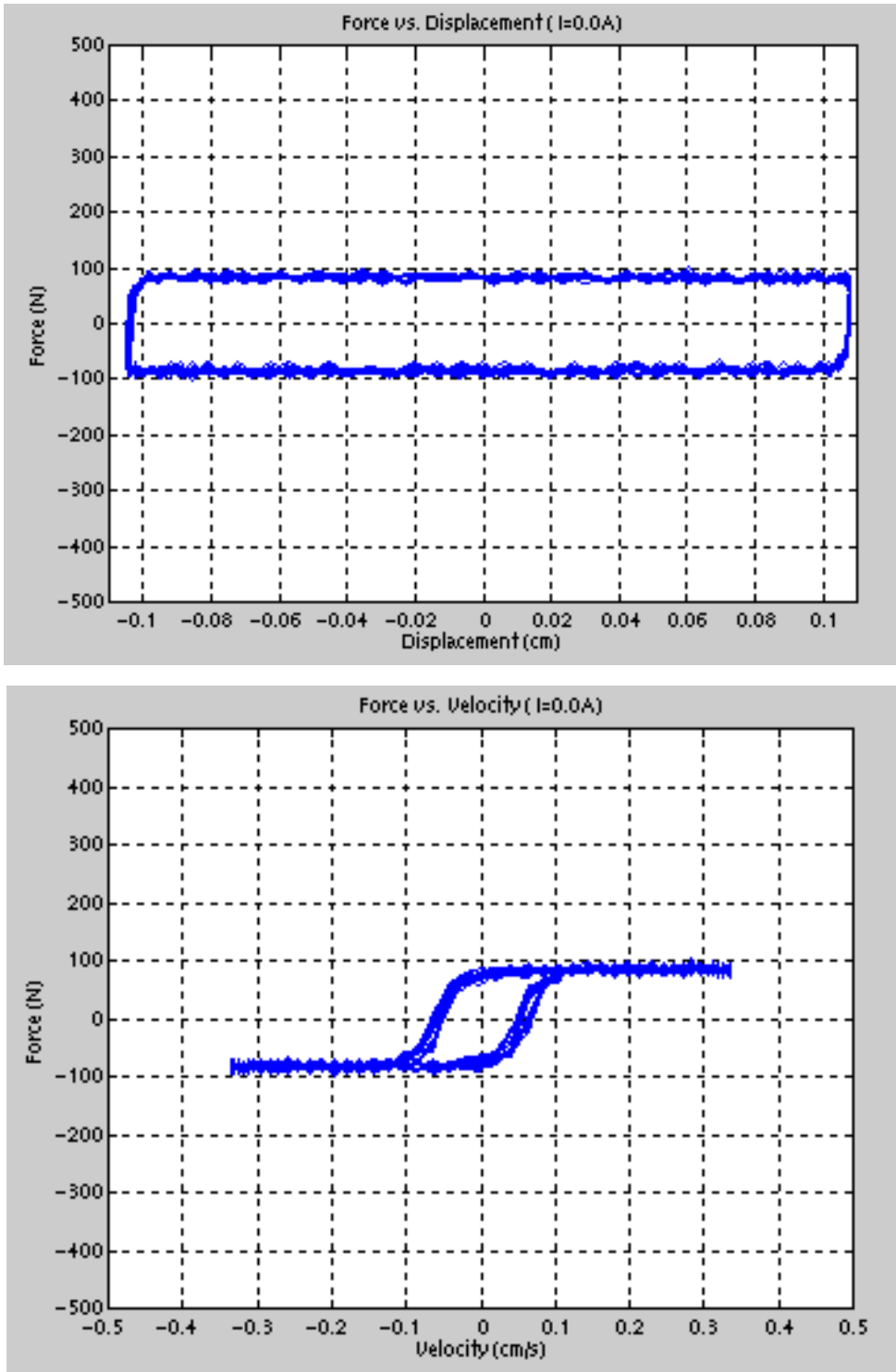


FIG. B-11. Current = 0.0 amps